Received: 20 December 2019 | Revised: 1 April 2020 | Accepted: 5 April 2020

DOI: 10.1002/app.49379

Journal of Applied Polymer Science WILEY

REVIEW

The search for enhanced dielectric strength of polymer-based dielectrics: A focused review on polymer nanocomposites

Daniel Q. Tan

Technion Israel Institute of Technology and Guangdong Technion Israel Institute of Technology, Shantou, China

Correspondence
Daniel Q. Tan, Technion Israel Institute of Technology and Guangdong Technion Israel Institute of Technology 241 Daxue Road, Jinping District, Shantou, Guangdong 515063, China.
Email: daniel.tan@gtiit.edu.cn

Funding information
Guangdong Science and Technology Department, Grant/Award Number: 2019A1515012056; Guangdong Technion-Israel Institute of Technology

Abstract

This report traces the leading scientific endeavors to enhance the dielectric strength of polymer dielectrics for energy storage and electrical insulation applications. Remarkable progress has occurred over the past 15 years through nanodielectric engineering involving inorganic nanofillers, coatings, and polymer matrices. This article highlights the challenges of dielectric polymers primarily toward capacitors and cable/wire insulation. It also summarizes several major technical approaches to enhance the dielectric strength of polymers and nanocomposites, including nanoparticle incorporation in polymers, filler-polymer interface engineering, and film surface coating. More attention is directed to interface contributions, including rational design of core-shell structures, use of low-dimensional fillers and thermally conducting fillers, and inorganic surface coating of polymer films. These efforts demonstrated the enhancement in dielectric strength by 40–160% when controlling the fillers below 5 wt% in polyvinylidenedifluoride (PVDF) composites. This article also discussed the possible dielectric mechanisms and the positive role of interfaces against charge transport traps for attaining higher breakdown strength. The investigation of low-dimensional filler/coating materials of high thermal conductivity can be key scientific subjects for future research.

KEYWORDS

2D boron nitride, dielectric strength, interface, nanofiller, polymer film

1 | INTRODUCTION

The growing demand for power electronics, energy storage, and extreme environmental systems provide an excellent platform for dielectrics and electrical insulation materials.[1–3] Dielectric polymers stand out particularly as incomparable materials for many electrical insulation and energy storage applications owing to their high dielectric strength, high voltage endurance, low dielectric loss, low equivalent series resistance, and a gradual failure mechanism. Their significant presence in various electrical technologies is shown in Figure 1. As for cable and wire insulation, the polymer coating protects the internal shielding and conductors, and from external moisture, mechanical, ultraviolet (UV) and ozone damage.[4,5] As for capacitor and tape insulation, polymer films/sheets are fundamental building blocks providing electrical charge build-up barriers and electrical current handling capability.[6–9]

Today, most of these applications make use of various commercial dielectric polymers and resins. One cannot overemphasize the importance of polymer films and their

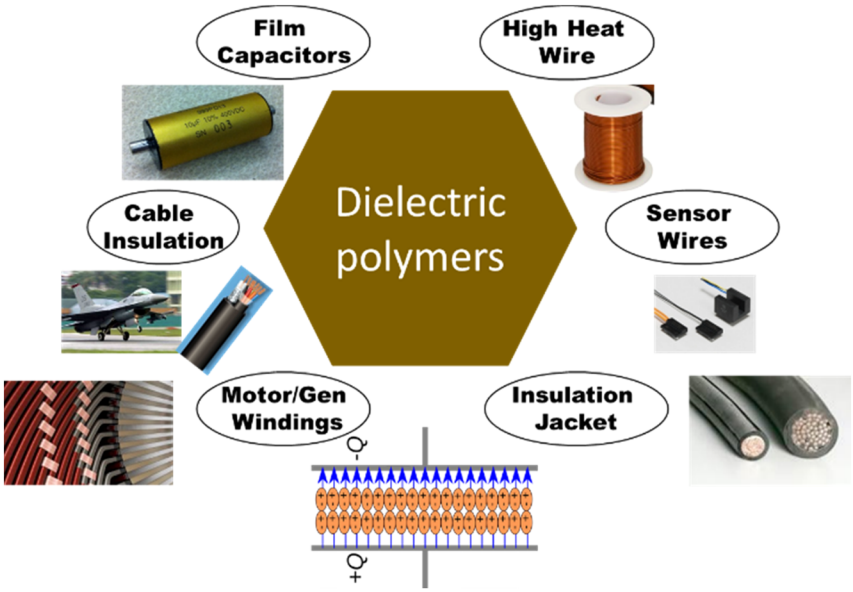

FIGURE 1 Typical applications of dielectric polymers in various electrical components and systems [Color figure can be viewed at wileyonlinelibrary.com]

improved properties for the relevant applications. Table 1 shows two typical applications of these materials (capacitor and cable/wire insulation).[10–16] The characteristic features and benefits of polymeric materials are listed in the table despite a broad range of operating conditions, under which the dielectric properties and breakdown mechanism vary dramatically from one application to another. In the technical area, the quantitative values regarding low, medium, and high values for a dielectric polymer film generally present as follows. Permittivity: <3.0 (low); 3.0–10.0 (medium); >10.0 (high); Dielectric loss: <0.002 (low); 0.002 ~ 0.02 (medium); >0.02 (high); DC dielectric strength: 150–300 kV/mm (low); 300–500 kV/mm (medium); >500 kV/mm (high); temperature: <85°C (low); 85–140°C (medium); >140°C (high). Dielectric strength, as one of the most desirable properties, can be assessed as breakdown strength for short term and voltage endurance for the long term. This intrinsic dielectric property primarily dominates the design rules of a dielectric material, to which the dielectric thickness, volumetric energy density (compactness), compositional tuning, and the manufacturing process should be defined accordingly. Although most of the performance metrics are more suitable for capacitor films, not all apply to cable/wire insulation films. The author investigated polytetrafluoro-ethylene (PTFE) and PerFluoroAlkoxy (PFA) polymer films expecting to predict their AC dielectric strength on cable/wire insulation based on the film DC breakdown strength. The uncertainty in the wire insulation manufacturing process and polymeric layer nonuniformity make it difficult to establish a direct relationship between the two performance parameters. Yet, a good polymer film such as PTFE and PFA should statistically possess a DC breakdown strength of >300 kV/mm and an AC breakdown voltage of >75 kV/mm to ensure an electrical endurance of insulated wires to 200 hr when tested at a voltage strength of 20 kV/mm.

More electric power application requires higher voltage stress, thinner insulation, and higher working temperature, which poses stringent requirements for dielectric polymers to possess higher dielectric strength and higher temperature ratings. Therefore, scientists and engineers have established many research projects dedicated to the development of new dielectric materials technology in the last two decades.[14–16] Nanodielectrics became the innovative subject, which aims to increase dielectric strength and dielectric constant of polymers and thus energy density.[17–20] Progress and challenges co-occur in materials innovation, property improvement, and film scale-up. For instance, the addition of fillers into a polymer can contribute significant enhancement of the local electric field in the composites and thus decreased dielectric strength, a phenomenon like electrical stress concentration in many cable accessories and motor end winding.[21] The pathway to the enhancement of dielectric strength was pretty bumpy despite success in increasing dielectric permittivity. And the scale-up production of mechanically flexible and robust polymer films of capacitor grade is quite tricky as well.[9,22] As a result, one can find some review papers addressing the progress in the enhancement of dielectric permittivity and energy density.[23–27] Some reviews only discuss the advancements in polyvinylidenedifluoride (PVDF)-based polymers that have high dielectric loss.[28,29] Some reviews discuss the partial discharge (PD) characteristics of polymer nanocomposites.[30] Some articles only review the

TABLE 1 Characteristics of commercial polymeric materials for electrical insulation and capacitor[10–16]

Polymers	Capacitor film performance metrics	Cable/Wire insulation	Benefits
PP (polypropylene)	High dielectric strength (800 kV/mm), low permittivity (2.2), low loss (0.0002), low temperature (85°C)	—	High current handling, large capacitance
PET (polyester)	High dielectric strength (~550 kV/mm), low permittivity (3.3), medium loss (0.005), low temperature (125°C)	—	Low cost
PC (polycarbonate)	High dielectric strength (~600 kV/mm), low permittivity (3.0), medium loss (0.0015), low temperature (125°C)	—	Higher temp. rating (125°C)
PPS (polyphenylene sulfide)	High dielectric strength (~550 kV/mm), low permittivity (3.0), low loss (0.0003), medium temperature (150°C)	—	Higher temp., lack of self-clearing
PTFE (polytetrafluoro-ethylene)	High dielectric strength (>650 kV/mm), low permittivity (2.1), low loss (0.0002), high temperature (260°C)	Wire insulation, AC dielectric strength (78 kV/mm)	High temp., voltage endurance
PEN (polyethylene naphthalate)	High dielectric strength (~550 kV/mm), low permittivity (3.1), medium loss (0.002), medium temperature (125°C)	—	Large capacitance
FPE (fluorene polyester)	High dielectric strength (~520 kV/mm), low permittivity (3.3), medium loss (0.003), high temperature (275°C)	Wire insulation	High temp. (>200°C), high current density
PEEK (polyetherether-ketone)	Medium dielectric strength (~430 kV/mm), low permittivity (3.2), medium loss (0.004), medium temperature (150°C)	Wire insulation	High temp., voltage endurance
PFA (PerFluoroAlkoxy)	Medium dielectric strength (~320 kV/mm), low permittivity (2.5), medium loss (0.0002), high temperature (250°C)	Wire insulation, AC dielectric strength (70 kV/mm)	High temp. And voltage endurance
PESU (polyether sulfone)	Medium dielectric strength (~400 kV/mm), low permittivity (3.5), medium loss (0.0035), high temperature (200°C)	—	Thinner tape or smaller capacitor size
PVDF based (poly(vinylidene fluoride))	High dielectric strength (600 kV/mm), high permittivity (11), high loss (0.02), low temperature (125°C)	—	Flexibility for processing
PEI (polyetherimide)	High dielectric strength (~550 kV/mm), low permittivity (3.2), medium loss (0.002), high temperature (200°C)	—	Overall performance
PI (polyimide)	Medium dielectric strength (~420), low permittivity (3.1), medium loss (0.0025), high temperature (300°C)	Wire insulation	High temp. Stability, lack of self-clearing

electrical treeing studies on how nanofillers mitigate insulation failure in nanocomposites in long-term breakdown regime.[31,32] Some articles review the thermoplastic elastomer blends for high voltage cable application, and electro-active polymers such as silicones for actuation application.[33,34]

Owing to the important significance of dielectric strength and recent good progresses, the present review focuses on short-term dielectric strength property of polymer films and nanofilled polymer dielectrics more favorable for capacitor applications. Here we will discuss the advantages and challenges of commercial polymer films, laboratory stage polymer dielectrics, and nanocomposite dielectrics toward capacitor and cable insulation in the last 15 years. Knowing the difficulty in unifying the development approach and performance metrics of polymeric materials for all applications, we will narrow down the review to polymeric materials modified by nanofillers or surface coating with a focus on the capacitor films. We will: (a) review the status of dielectric material research toward dielectric strength enhancement for capacitor and cable applications; (b) illustrate the endeavor via three routes: adding nanoparticles in polymers, engineering filler-polymer interfaces, and coating film surfaces; and (c) indicate the development needs and future perspective for improving dielectric film technology.

2 | ADVANTAGES AND CHALLENGES OF POLYMER DIELECTRICS—HISTORICAL PERSPECTIVE

2.1 | Unfavorable decrease in dielectric strength

Dielectric properties are material thickness dependent. Thicker dielectric materials mostly exhibit a lowered dielectric strength, as shown in Figure 2a.[35] The model and experimental evidence suggest bipolar charge injection and the formation of charge packets under higher electric fields. The thickness dependence is the result of charge dynamics in the material. If possible, thinner dielectric materials withstanding higher voltages are preferable. Thinner dielectric films give rise to smaller volumes of the insulation system and capacitor components. The effort to create thin films, however, is not always suitable for high-performance capacitor technology because of various material and processing requirements. Unlike the exceptional case of silicon oxide being grown almost perfectly on a silicon single crystal, where dielectric strength increases with decreasing thickness down to 20 nm, most dielectric materials are affected by processing and defects. As a result, dielectric strength ceases its monotonous increase with decreasing thickness of the dielectric film. For many polymer films, the thickness threshold is below 10 μm. Figure 2b shows the commonality of reduction in the dielectric strength of several polymer films of skinny gauge, which severely hinders the dielectric properties of ultrathin films and their application in high energy density components.[16,36,37] For example, biaxially stretched polypropylene BOPP, benefiting from its high dielectric strength and low dielectric loss, lost its dielectric strength considerably when the film evolved to ultra-thin gauge. High-temperature polymers such as PTFE and imides are also subject to similar reduction. Thinner films exhibit more surface defects (e.g., pits, dimples, contaminants, roughness, wrinkles, and variable thickness), which may easily subject the thin film to local plasma erosion or breakdown, resulting in a wide breakdown strength distribution.[38–40] Recent computer simulations have even demonstrated the possibility of electrical failure in this situation.[41] Charge injection at the metal-dielectric interface is often a primary failure mechanism and is still an important topic of concern for dielectric materials and components.

2.2 | Favorable dielectric materials

To produce high performance, favorable dielectrics, scientists worldwide have conducted an assessment of various commercial polymer films, syntheses of new polymer

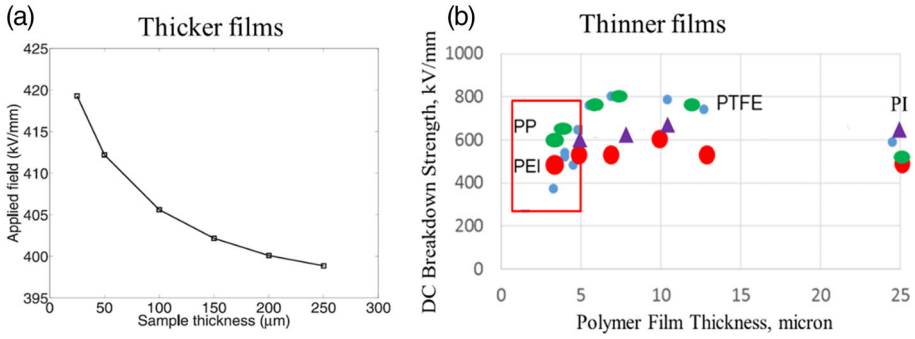

FIGURE 2 (a) Empirical thickness dependence of DC dielectric strength of thicker materials; Reproduced with permission.[35] Copyright © 2012 AIP Publishing. (b) Thickness dependence of DC dielectric strength of thinner films (metallized film electrodes for PP, PTFE and ball-plan electrodes for PEI and PI) [Color figure can be viewed at wileyonlinelibrary.com]

TABLE 2 High temperature and high-performance polymer films[16,49,51,53,57,58]

Type	Polymer films	Advantage	Challenges
I—Commer-cial film	PEI	Overall property and film thermal scalability (0.1% shrinkage)	High cost (>$200/kg) and lower dielectric strength comparing with BOPP (800 kV/mm)
	PEN	Scalability in manufacturing and thinner gauge (2.5 μm)	Dielectric loss (>0.001), cost (>$200/kg)
	PEEK	Scalability in manufacturing of pure film and inorganic filled composites (6 μm)	Low dielectric loss (>0.001), dimensional change (>) and lower dielectric strength (430 kV/mm)
	PPS	Low dielectric loss (0.0003) and thin gauge (<1 μm)	Lack of self-clearing and lower temperature (150°C)
	PI	Scalability in manufacturing and high temperature (300°C)	Lack of self-clearing and higher dielectric loss (0.002)
	PTFE	Low dielectric loss (<0.001), high dielectric strength (>650 kV/mm) and high temperature (260°C)	High cost (not for sale) and low dielectric constant (2.1), mechanical strength lower than BOPP
	FPE	High temperature (275°C)	Solution coating process and high cost (>$200/kg)
II—Lab research dielectric	Polyurea	High dielectric strength (800 kV/mm), high temperature (180°C),	High dielectric loss (0.005), film process scalability
	Polythiourea	High dielectric strength (1,000 kV/mm), high dielectric constant (4.5)	High dielectric loss (0.005), cost, and film process scalability
	Imide based BTDA-HAD or BTDA-HK511	Medium high dielectric constant (7.8), high dielectric strength (>670 kV/mm)	Higher loss (0.007), film process scalability
	CN-PEI	High temperature (220°C), high dielectric constant (4.7)	Film process scalability
	Organometallic polymer	High dielectric constant (10–30)	Higher dielectric loss (>0.01), low breakdown strength (<400 kV/mm), film scalability
	Modified PP	Higher dielectric constant (3.3–4.5) and high dielectric strength (>600 kV/mm)	Film process scalability and induced polarization loss
	Acrylate PML	High dielectric strength (1,000 kV/mm)	Too thin (<0.5 μm, no stand-alone film
	PHONDI	Medium dielectric constant (3.2) and temperature (150°C)	High dielectric loss (0.007) and medium dielectric strength (350 kV/mm)
III—Nano-composite	PEEK	Increased dielectric constant and proven composite films	Lower dielectric strength (<300 kV/mm)
	PVDF or PVDF copolymer	Higher dielectric constant (10–80) and mechanical strength	High dielectric loss (0.02), low temperature (125°C), film process scalability
	FPE	High temperature (275°C), and dielectric constant after adding fillers	Low dielectric strength (<300 kV/mm) and mechanical strength, film process scalability
	PEI	Higher dielectric constant after adding low filler concentration	Lower mechanical strength containing fillers above 10 wt%, film process scalability

(Continues)

TABLE 2 (Continued)

Type	Polymer films	Advantage	Challenges
		(>4), high dielectric strength (500 kV/mm)	
	PEEU, poly(arylene ether urea)	Higher dielectric constant (>7), high dielectric strength (>600 kV/mm)	High dielectric loss (0.01),
	PI	Higher dielectric constant (>5) after adding fillers	Low dielectric strength (<300 kV/mm) and mechanical strength
	Silicone	Higher dielectric constant (>5)	Low dielectric strength (<300 kV/mm) and mechanical strength, thick film
	c-BCB, cross-linked divinyl -tetramethyldi-siloxane-bis (benzo- cyclobutene	Lower dielectric loss (0.001) and electrical conduction, and stable breakdown strength (400 kV/mm) up to 250°C	Low mechanical strength, film process scalability
	PMMA, poly(methyl methacrylate)	High dielectric constant (5–20),	High dielectric loss (0.02–0.1), low dielectric strength (20 kV/mm), low temperature (105°C)
	PE	Reduced conductivity, high voltage endurance for insulation	Film process scalability and low filler uniformity
	Cellulose acetate, cyanoethyl	High dielectric constant (>20), OFETs dielectric	High dielectric loss (>0.02) and low mechanical strength

dielectrics, and engineering of nanodielectric composites. Table 2 shows a compilation of these materials along with their advantages and challenges with a focus on polymer films for capacitor applications. Commercial high-temperature films such as PTFE, polyetherimide (PEI), polyethylene naphthalate (PEN), fluorene polyester (FPE), and polyimide (PI) are mostly expensive.[8,42–45] Some of them possess lower dielectric strength, higher dielectric loss or lack of self-clearing capability, which are desirable properties for high-performance capacitors. A second type of dielectrics is being developed in research laboratories because they hold promise for more exceptional dielectric properties and high-temperature ratings. Their challenges remain to be dielectric strength, dielectric loss, and high-quality film processing.[46–58] The third type of dielectric material underway is nanocomposites that leverage a high-performance dielectric polymer to host proper nanofillers using ingenuous processing methods. The challenges are associated with low dielectric strength, mechanical strength, and scale-up of composite films.[59–63] Therefore, the choice of dielectric materials with excellent overall properties and processes is minimal, considering the requirements in dielectric loss, dielectric strength, harmful solvents, heat shrinkage, and film-forming ability, etc. Better ideas are highly needed to fulfill high dielectric strength, low dielectric loss, and innovative material processes.

2.3 | Dielectric breakdown mechanism classification

Dielectric breakdown involves complicated mechanisms, and this is especially true for polymer-based dielectric and nanocomposite materials. Depending on the dielectric material constituents, electrical conductivity, thermal conductivity, interfaces, surface imperfection, and thickness, the breakdown mechanism can be much different.[64] The dielectric breakdown regime in terms of time scale being described in several versions now is revised to exhibit in Figure 3a for this review. For time scales longer than minutes, the so-called long-term dielectric breakdown dominates the degradation mechanisms, which are from oxygen migration, electrical trees, and water trees. This mechanism usually occurs in thick insulation materials in specific environmental situations during voltage endurance events. The dielectric breakdown behaviors of the insulation materials are dependent on electrical stress conditions, chemical structures, and their application environment, such as temperature, etc, which can cause electrical charge mobility, and increased conductivity. Even in polymeric dielectrics, such as polyethylene having a wide bandgap (Egap∼8.8 eV), a low overall charge mobility (10^{-6} cm/Vs) persists even in the absence of traps, probably due to disorder localization in the amorphous part of the polymer.[64–66] For polymer dielectrics,

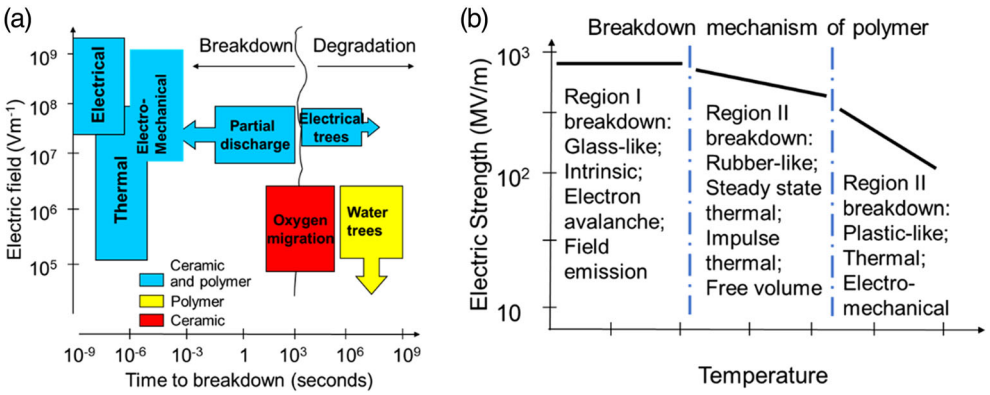

FIGURE 3 (a) Schematic outline of dielectric breakdown mechanism in various dielectric materials,[228] (b) the temperature dependence of dielectric strength of linear polymers [Color figure can be viewed at wileyonlinelibrary.com]

Nunes and Shaw[67] mainly discussed the behavior of DC trees caused by space charge accumulation with the nature of carrier injection and trapping in polymers. Ieda[68] addressed the breakdown processes from the standpoint of the inherent properties of polymers, such as chemical structure, structural irregularities, the presence of additives, molecular motion, and so on. The common breakdown mechanisms such as electron avalanche, thermal runaway, and electromechanical failure can be accordingly sketched in Figure 3b to explain the breakdown behaviors of polymeric materials. At very low temperatures, electron avalanche dominates the failure mechanism that displays negative thickness dependence and positive temperature dependence of the electric field. Thermal breakdown often results from the local temperature rise and hot electrons or holes as the local temperature is a direct function of location and time, and the local temperature defines the energy distribution of conduction electrons or holes at each location. The combined stresses from high frequency, high voltage, and high temperature at low pressure pose severe problems to insulation life and the full system's reliability. The breakdown behavior of insulation under these environments is yet not fully understood.[69–72]

For time scales of about seconds or less, the short-term breakdown events are a more complicated subject, where PD or plasma corona, electromechanical stressing, thermal, and electrical breakdown are responsible mechanisms. As an example, glass ceramics electrically degrade related to several factors, such as degree of crystallinity, accumulation of bulk charge, interfacial area, crystal size, and interface number. Due to the significant role of interfaces in charge trapping, interface properties such as amorphous or intermediate phases within the glass-ceramics significantly affect the dielectric strength.[73] Polymers and polymer composites contain various molecular chains, regions, interfaces, and surfaces; hence the controlling factors can be even more complicated.

3 | ENDEAVORS TO ENHANCE DIELECTRIC STRENGTH

Since the appearance of the nanodielectric concept, researchers have attempted to figure out how to raise the dielectric strength of materials (proportional to voltage for a specific thickness) and the energy density of capacitors (proportional to the square of dielectric strength). Looking back in the history, one can see three different major methodologies on the endeavor: adding nanoparticles in polymers, engineering filler-polymer interfaces, and coating film surfaces.

3.1 | Adding nanoparticles in polymers

Filling nanoparticles in polymers to manipulate the composite structure and properties is the core content in nanodielectric researches investigating the dielectric phenomena and electric insulation. Increasing dielectric permittivity and corona resistance of the host polymers has easily accomplished. Yet the enhancement of the dielectric strength through nanodielectric engineering has gone through a long history. Cao et al.[20,74] from GE Global Research attempted to improve the overall dielectric properties of polymers by adding various nanoceramic particles 15 years ago. No significant increase was achieved by merely adding nanofillers for loadings up to 10 wt% as shown in Figure 4a. The present author working with the same group subsequently investigated various nanofillers working with thermoplastic polymers such as polypropylene (PP), PEI, cellulose cyanoethyl, and PVDF since 2005.[75,76] It turns out that enhancing dielectric strength by merely filling with nanoparticles (SiO_2 and Al_2O_3, TiO_2, $BaTiO_3$) along with additional functionalization is still not a satisfied solution. Working with various polymer processing methods such as compression molding, solvent casting, melt extrusion, and in-situ polymerization, the team found it most rewarding to

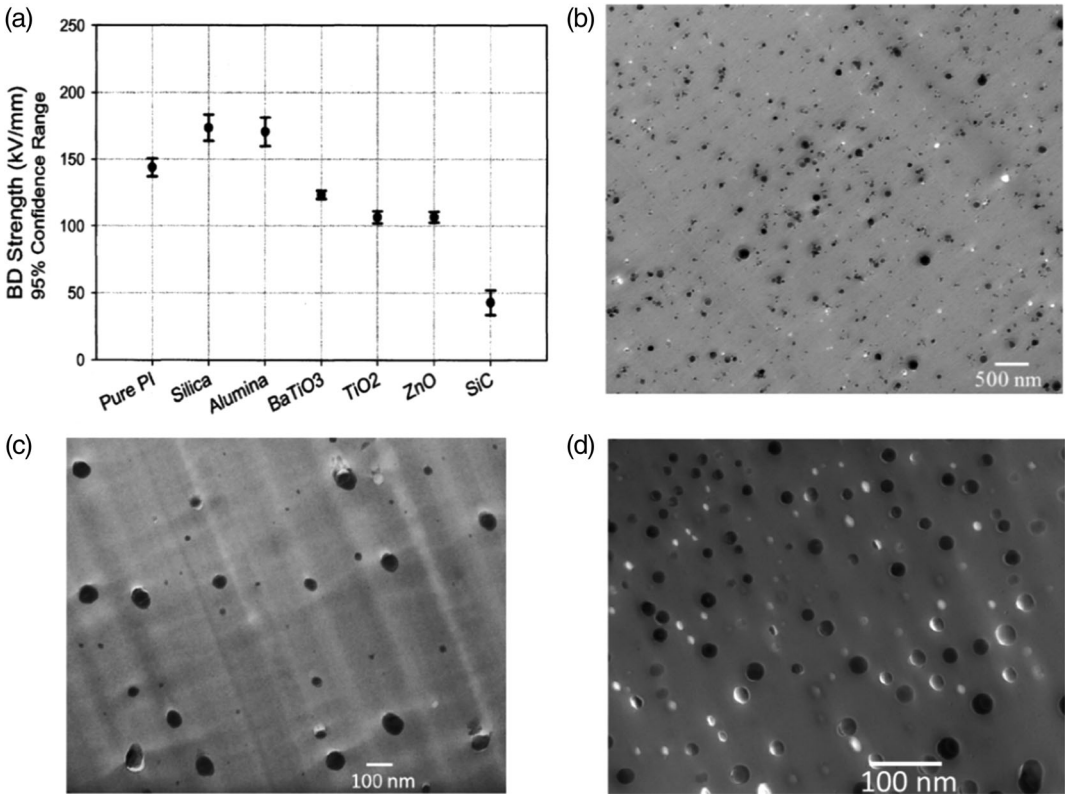

FIGURE 4 (a) AC breakdown strengths for PI with various nanofillers at 5 wt% loading. The tests were performed with 500 V/s ramp rate on 25 μm thick samples. The remarkably low breakdown strength of SiC nanocomposites may be caused by the aggregation of SiC nanoparticles. Reproduced with permission.[74] Copyright © 2004, IEEE. TEM image for dry 45 nm Al_2O_3 mixed in PEI matrix (b) 5 wt% TiO_2 nanoparticles dispersed in a PPS film using a self-assembled in-situ particle precipitation process (c), and 5 vol% SiO_2 dispersed in polyamic acid by in-situ polymerization (d). (Open access, 75)

use in-situ polymerization. Good nanoparticle dispersion and good particle-polymer interface bonding are achieved, as shown in Figure 4b–d.

Adding inorganic fillers is surely a generic method for the dielectric improvement of electrical insulation materials.[11,77,78] In 2005, Roy et al. *from the RPI group* reported that the incorporation of SiO_2 nanoparticles into thermoset cable insulation XLPE increased the dielectric strength compared with the base polymer.[79] This increase appears when measuring the dielectric strength using a tip electrode poking into the samples, which was not the same as most test electrodes in parallel metal fixtures. The divergent field associated with the tip electrode remains localized at the tip of the growing tree during the whole breakdown process.[80] It was postulated that nanoparticles prevent space charge accumulation in the nanocomposite volume. The same group observed the similar enhancement after carefully controlling the processing conditions when making nanocomposites.[81] Tanaka and Tuncer also reported a small percentage increase in dielectric strength in nanocomposites.[82,83] Although insulating materials with high corona resistance and tracking resistance were also developed, demonstrating the pronounced effect of nano Al_2O_3 and TiO_2, yet, their improvement is not as effective as micron-sized mica and progress in this subject remains slow.[84] Partial discharge can generate high energy electrons, ultraviolet rays, local high temperature, and active ions. The nanofillers tend to resist the high energy damage and thus increase the discharge resistance performance of the dielectric.[85] Ismail et al. summarized a list of thermoplastic elastomer (TPE) systems and their composites with common nanofillers useful for electrical insulation applications.[33] Various types of TPE blends increasingly find acceptance in HV insulators; however minimal publications and improvement reported the improvement of the electrical insulation performance of nanofilled TPEs. Scientists found that adding MgO nanoparticles in blended PP and polyolefin elastomer can suppress the accumulation of space charge and to increase the breakdown strength. Yet, the scale-up of TPE nanocomposites for power cables insulation requires better filler dispersion, understanding the property variation under combined voltage and temperature, the behavior of nanodielectrics to long-term operation, the manufacture of recyclable materials.[86]

Unlike highly resistive oxides such as Al_2O_3, SiO_2, and $BaTiO_3$, semiconductor oxides like ZnO, insulating nitrides like AlN, Si_3N_4, and BN have also been considered as additives in the rubber industry, electrical stress control for HV insulation and electronic packaging application to handle the heat dissipation.[87] With increasing the difference in dielectric constant or electrical conductivity between the fillers and polymer matrix, the field distortion considerably rises and the local field enhancement becomes greater. The choice and incorporation of the fillers must be careful to modify the breakdown field of a composite significantly. Fillers with low-K, low electrical conductivity, and high thermal conductivity appear to be more desirable for the achievement of high breakdown electric field in a composite. An example is demonstrated by Andritsch et al.[88] who observed an increase in DC dielectric strength of an epoxy composite and attributed it to the strong interfacial bonding between polymers and BN fillers. Lee et al.[89] described an example of the enhancement in nano-DC-XLPE cable insulation materials compared with conventional AC-XLPE and DC-XLPE. Paramane et al. reported the surface treatment effect of nanoparticles on water tree growth resistance in XLPE, the prolonged tree initiation and propagation, and improved voltage endurance and PD in epoxy.[90] Li et al.[91] summarized that the DC dielectric strength enhancement became more feasible when nanoparticle content lies between 0.05 and 2 wt%, which is associated with the transitional region surrounding the nanoparticles. Using micron-size particles, it is not possible to see the improvement across the board, as shown in Figure 5.[92–97]

Nevertheless, many nanodielectric investigations in the first 10 years neither confirmed nor observed the enhancement of dielectric strength in thermoset plastic-based nanocomposites.[97–102] Notably, minimal results reported encouragement in filled thermoplastic thin films. These studies clearly showed that only performing organic functionalization on nanofillers has a minimal role. What puzzled people more is whether or not nanofillers can play a predominant role in this endeavor.

3.2 | Engineering filler-polymer interfaces

After 5+ years of stagnation at less than 50% enhancement and its uncertainty, researchers saw a new horizon by engineering filler-polymer interfaces.[103–105] Besides emphasizing the distribution/dispersion of fillers themselves, researchers paid more attention to the role and ingenious design of filler-polymer interfaces, an additional third phase in nanocomposite systems. The interfacial phase can occupy >50% by its volume ratio and thus can have a significant impact on the overall performance of nanocomposites and their devices. According to Schadler,[106] the size of the interface region can be as large as 250 nm and depends on the degree of interaction between the polymer and the nanoparticle. Several phenomenological models tried to explain the contribution of the interface, including induced local orientation of CH_2–CF_2 dipoles, exchange coupling effects of the interface, and Maxwell–Wagner–Sillars polarization.[107–109] Recently, direct detection of the local polarization at the interface in very thin film samples was reported based on the modified Kelvin probe force microscope (KPFM).[110,111] Figure 6 shows the interfacial polarization model and the induced surface potential difference associated with the matrix/particle interface region in ferroelectric polymer nanocomposites. By considering the

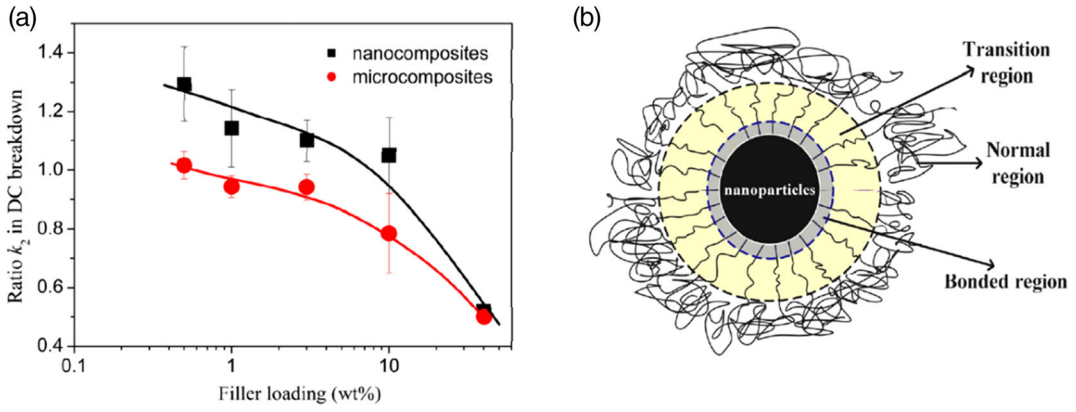

FIGURE 5 (a) Ratio k_2 in DC breakdown strength versus nano/micro-filler loading for polymer composites containing various treated fillers. All breakdown tests were performed in silicone oil at 303 K with a ramp rate of 500 V/s. The thickness of specimens was ranging from 50 to 500 μm. (b) Schematic of multi-region structure around spherical nanoparticles. Reproduced with permission.[91] Copyright © 2010, IEEE [Color figure can be viewed at wileyonlinelibrary.com]

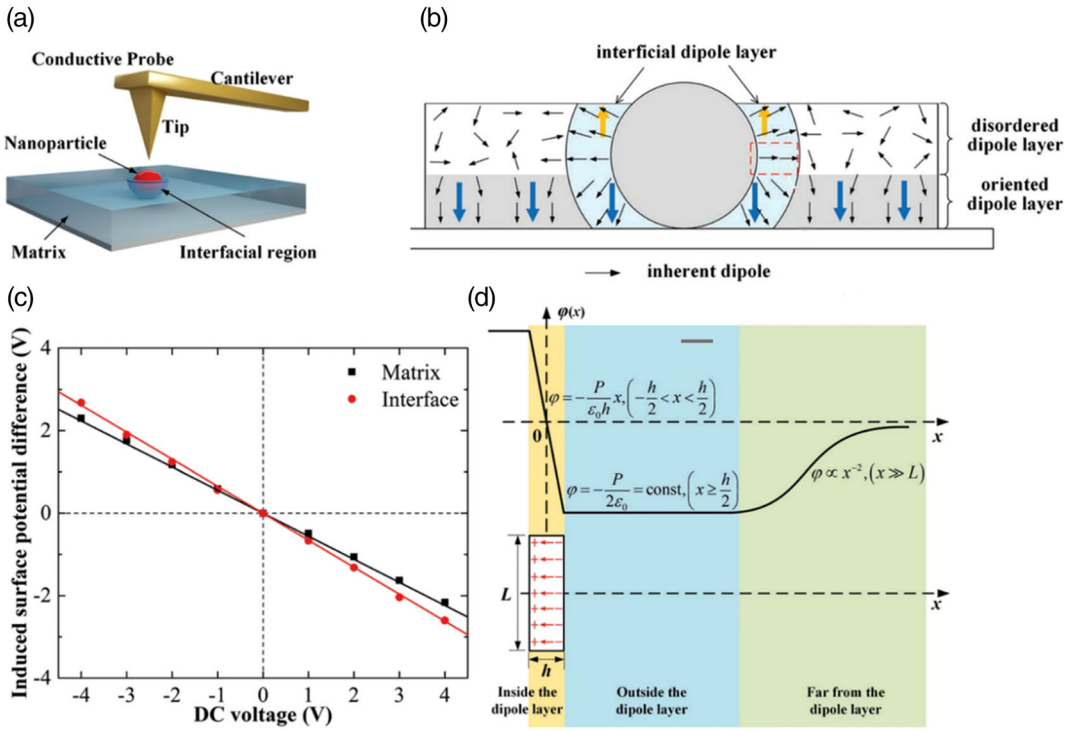

FIGURE 6 (a) The schematic diagram of the conductive AFM testing setup; (b) The structural model of P(VDF-TrFE)/BT nanocomposite spin-coated on Au substrate; (c) The induced surface potential difference under different DC voltages of P(VDF-TrFE) embedded with BT nanoparticles; (d) The electric potential at a distance *x* from the dipole layer with finite length and thickness according to Gauss's law.[111] This is an Open Access article permitting unrestricted use [Color figure can be viewed at wileyonlinelibrary.com]

enhanced interface electric polarization, one can explain the considerable discrepancy between the simulated value and experimental results at a low loading fraction. The properties of the interface region must achieve desirable capabilities of nanodielectric composites, which poses excellent significance to both capacitor and cable insulation. Toward control and engineering filler-polymer interfaces, there appear three progressive efforts: core-shell nanoparticles, conducting fillers of low-loading, and low-dimensional thermally conductive fillers.

3.2.1 | Core-shell nanoparticle design

A dielectric mismatch between nanofillers and polymer matrix is known to cause local electric field stress at the filler-polymer interfaces and significant reduction of the breakdown strength. To alleviate the localized high field concentration, core-shell structured fillers exhibit a gradient property. The core-shell particle concept may have originated from structured composite particles consisting of one at the center as a core surrounded by the second as a shell.[112–114] Smart properties are the most desirable characteristics that allow this class of polymer to be used in various applications, particularly in biomedicine as drug delivery systems. Wang et al.[115] conducted an early investigation on the core-shell concept of coating nanofillers with an inorganic shell. Systematic computer modeling showed that core-shell structures of filler particles provide an effective way to mitigate the local electric field concentration in dielectric composites, improving dielectric breakdown strength and energy density of the composites (Figure 7). The authors suggested to use a low shell dielectric constant and thick shell coating as an optimal design for core-shell fillers. Experimentally, the effectiveness of core-shell structures on dielectric properties was investigated by various research laboratories. Many of these constructed the fillers using $BaTiO_3$ (BT) particles as the high dielectric constant core and other inorganic or organic dielectrics as the low dielectric constant shell, including Al_2O_3, SiO_2, TiO_2.[116–119] For example, Li et al.[119] reported an in-situ polymerization technique to synthesize polypropylene-$BaTiO_3$ nanocomposites. $BaTiO_3$ nanoparticles were coated with an Al_2O_3 shell to accommodate the significant permittivity contrast between the $BaTiO_3$ nanoparticles (50–6,000) and the polypropylene (2.2). The internal conduction loss along the interface is then effectively mitigated through this method; the improvement in dielectric strength also appeared in some composite systems.[119–124] Alternative shell materials and fillers of lower loading fraction are yet to play a positive role for the demonstration of better results.

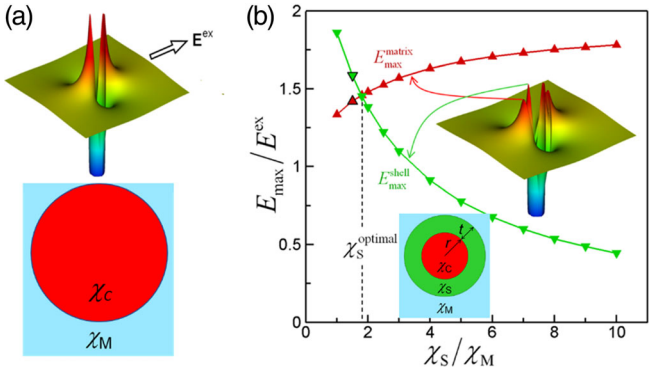

FIGURE 7 (a) Filler particle without core-shell structure embedded in matrix with χ_M:χ_C = 1:100. Without shell, the field is more concentrated at the interface (more spiky); (b) Effect of shell dielectric susceptibility on local electric field concentration in core-shell filled composite with χ_M:χ_C = 1:100 and t/r = 2:3. Maximum local electric field magnitudes concentrated in the matrix (red) and shell (green) as a function of χ_S. Inset corresponds to data point χ_M:χ_C = 1.5:1 as highlighted by black triangles. Reproduced with permission.[115] Copyright © 2011, AIP Publishing [Color figure can be viewed at wileyonlinelibrary.com]

3.2.2 | Conducting fillers of low loading

The second type of effort was attempted by utilizing conducting fillers such as nano Ag, nano Pd, graphene, nano ZnO and semiconductor particles as an unconventional method. Because their existence may form conducting-insulating interfaces, the traps for electrical charges may become a good thing that delays the charge transport.[103,125–129] An extremely low concentration (0.005 wt%) of graphene in low-density polyethylene (LDPE) rendered an excellent demonstration. Li et al.[130] discovered that the minute loading of graphene resulted in lower dc conductivity of about 3 orders of magnitude and a higher breakdown strength of 12.8% as shown in Figure 8. Much fewer space charges accumulate in the bulk of the 0.005 wt% grapheme/LDPE composite, which is attributed to the polymer-graphene interaction zones suppressing charge carrier transport. The homocharges near the electrodes reduce the effective field at the electrode-polymer interface, enhance the potential barrier for Schottky injection of homocharges from the electrodes into the polymer. These encouraging results might

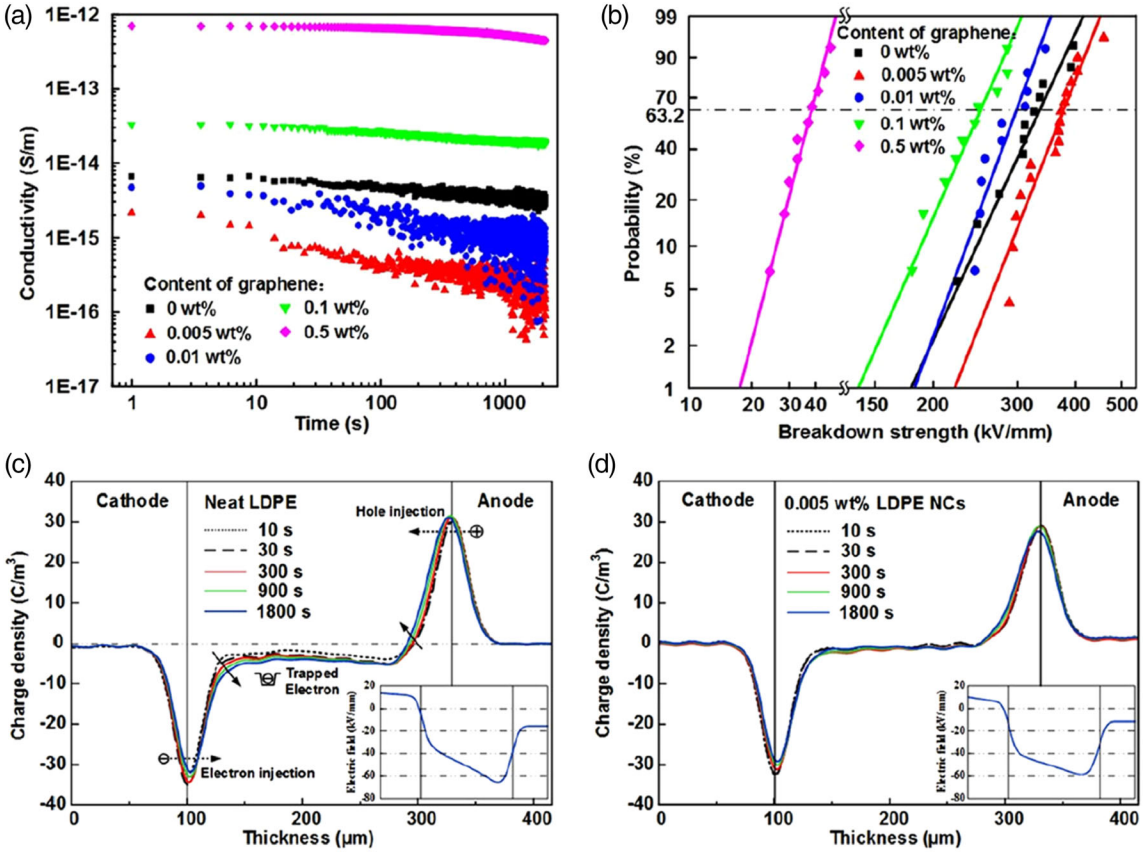

FIGURE 8 (a) DC conductivity of LDPE/graphene nanocomposites as a function of polarization time under 10 kV/mm. (b) Weibull distribution of dc breakdown strength of LDPE/graphene nanocomposites. (c) Space charge behaviors neat LDPE; and (d) 0.005 wt% LDPE/graphene under 50 kV/mm measured by PEA method.[130] This is an Open Access article permitting unrestricted use [Color figure can be viewed at wileyonlinelibrary.com]

have changed the conventional view of electrical conducting fillers that cause higher dielectric loss and electrical conductivity. Instead, the low-loading of graphene may act as deep traps to capture charges and enable higher voltage withstanding capability.

Another example filler for improving the dielectric strength is ZnO. At low loading fraction (3 vol%), the resistivity of the ZnO filled PVDF composites increased.[131] Higher loading causes a typical decrease in resistivity, as shown in Figure 9. Enhancement in breakdown strength of a PVDF composite is also observed, which is surprising. The author proposed that the discrepancy in physics and chemistry between the filler and the polymer matrix could form a charged interface region with a relatively low resistivity. The generated charges under the applied electric field will enter this region and get immobilized to some extent, which delays the formation of the conduction path. Too much conductive ZnO cannot be added because no insulating shell exists against an electric field. It is to be pointed out that the induced enhancement by conducting fillers is still limited and should be wisely leveraged in combination with other dielectric materials for a better outcome.

One of the clever designs is to coat the conductive particles with a non-conductive material forming a varistor particle structure where the non-conductive shell provides a barrier potential against electron transport. Conventionally, the conductive ZnO particles are isolated by small amounts of oxides of Bi, Sb, Co, Ni, or Mn dopants, creating a potential barrier between ZnO grains. These heterogeneous grain boundary junctions act as trap regions for electron accumulation and a barrier potential that is only lowered by a high electric field resulting in nonohmic I–V characteristics.[132–134] ZnO fillers or heterojunction fillers were also previously incorporated into electrical insulating polymers at more than 30 wt% to enable the operation of nonlinear electrostatic discharge devices, field gradient insulation composites, and electromagnetic shielding composites.[135–137]

The ZnO embedded polymer possesses field-dependent resistivity enabling electric stress control in high voltage apparatus. This nonlinearity has a lot to do with the ZnO filler surface barrier. Various research studies demonstrated that the diffusion of oxygen into grain boundary junctions is very effective in converting a conductive ZnO sample to a less conductive resistor with high nonlinear characteristics (Figure 10a).[139,140] The advantageous role of heterostructured semiconductive nanoparticles at lower loading fraction should be carefully investigated. Without a shell, the addition of ZnO in a polystyrene resin results in the decrease in surface resistivity of the nanocomposites with increasing ZnO concentration.[140] Similarly, semiconductive ZnS causes

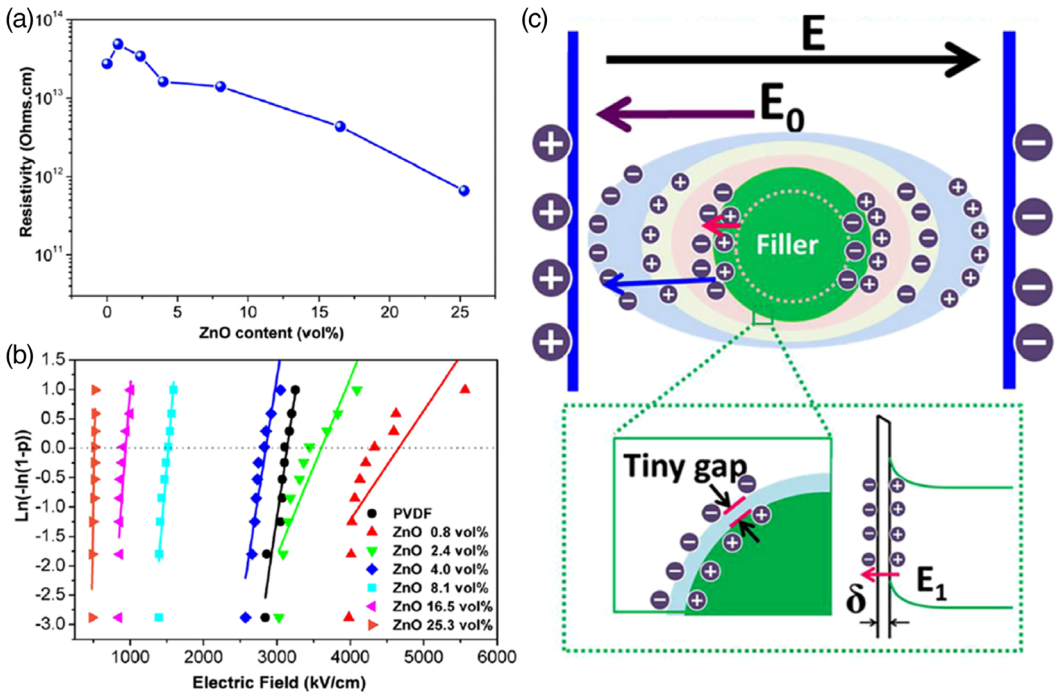

FIGURE 9 (a) Variation of resistivity of ZnO/PVDF nanocomposites with the filler content. (b) Weibull distribution of breakdown strength of ZnO/PVDF. (c) Schematic image of the distribution of charges and the formed internal electrical field induced by the applied electric field. Reproduced with permission.[131] Copyright © 2017, AIP Publishing [Color figure can be viewed at wileyonlinelibrary.com]

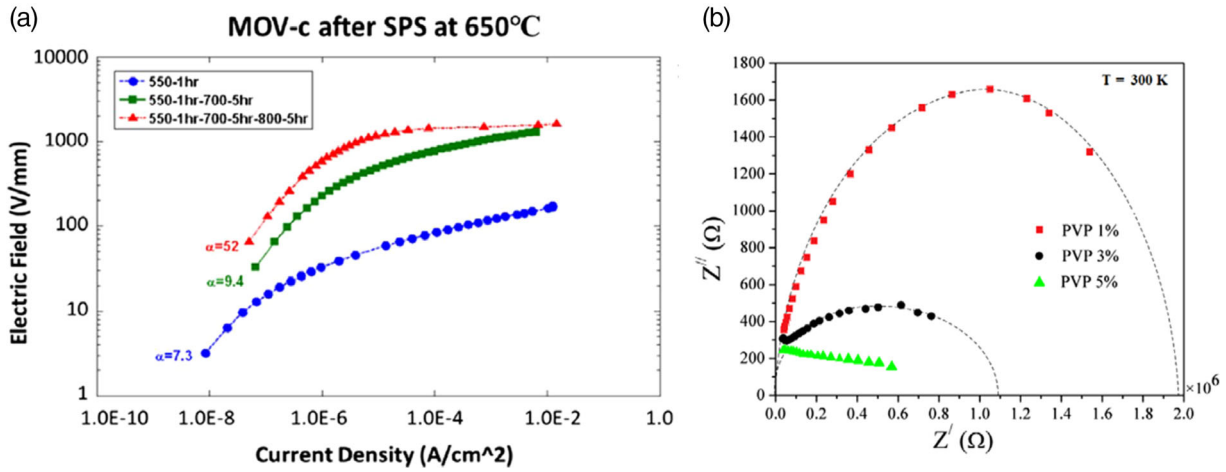

FIGURE 10 (a) Electrical properties of Metal oxide varistor (MOV-c) after SPS densification treatment and subsequent oxidation at various temperatures, (b) Niquist diagram of PVP-capped ZnS nanoparticles.[139,140] This is an Open Access article permitting unrestricted use [Color figure can be viewed at wileyonlinelibrary.com]

polymer composites to be more conductive. If ZnS nanoparticles were capped with a polyvinylpyrrolidone (PVP) shell, the reduced conductivity was achievable in samples with 1 and 3% concentration of PVP, where a small DC conductivity originated from low numbers of free charges. The sample containing 5% of PVP coating appears to keep nearly all free charges or ions trapped and exhibits no DC conductivity (Figure 10b).[140]

A modification of the ZnS nanofillers with additional oxygen further results in significantly enhanced breakdown strength and energy density in comparison with pure PVDF. High-performance dielectric polymers were prepared consisting of ZnS:O nanoparticles (ZSO NPs) with isoelectronic traps and PVDF matrix. Compared with pure PVDF and PVDF/ZnS composites, the energy density and breakdown strength for polymer nanocomposites with surface modified ZSO fillers are enhanced, as shown in Figure 11.[142] The transportation of carriers under an applied voltage is related to the delayed formation of a conduction path by the charged interfaces. Besides, the electric field imposed on the composites is reduced by the internal micro-electric field.[142,143]

Recently, the ZnO surface structure was further engineered to form a non-conductive junction and results in substantially enhanced dielectric breakdown strength and energy density. It was conjectured that charge carriers were captured and confined in the composite through the potential barrier formed at the heterojunctions of ZnO-ZnS nanoparticles. The space charge accumulation at the filler-matrix interface is relieved, and the concentration of the local electric field is weakened.[144]

3.2.3 | Low-dimensional thermally conductive fillers

To further augment the dielectric strength of polymer films, researchers have widely explored the effect of low-dimensional fillers and the corresponding core-shell structures.[145–149] 2D or 1D fillers possess high aspect ratios, less aggregation, high thermal conductivity, and lower loading fraction for the percolation threshold.[150,151] As a result, the risk of decreasing dielectric strength due to high loading is minimal. Among various 2D platelets, hexagonal boron nitride nanosheet (BNNS) present itself a preferred filler promising a new horizon for enhanced film dielectric strengths and energy storage in a wide temperature range.[152,153] The crosslinked polymer nanocomposites also exhibit better dielectric properties that are likely attributing to the BN heat dissipation capability. This BN-associated advantageous behavior resonated with earlier positive results by Andritsch et al.,[77] and 2D Montmorillonite reported by Fillery et al.[154] When using 1D fillers such as BaTiO3, SrTiO3, BaxSr1-*x*TiO3, and TiO2 nanofibers as the core, the advantage of improvement in dielectric strength also prevailed.[124,155–161]

Recently, more encouraging results exhibited when leveraging a novel core-shell filler construction comprising BNNS.[162–165] BNNSs functionalized with edge-hydroxylation led to a good dispersion and compatibility of BNNSs/polymer, leading to an increment of 46.6% in breakdown strength compared with PVDF/BNNSs nanocomposites. Figure 12 shows the chemical process and functionalized BNNS fillers in PVDF polymer and their effect on the dielectric strength. The better dielectric

and mechanical properties observed in PVDF/EOH-BNNSs nanocomposites may be related to the minimal insertion of impurities and the unique nature of the in-plane crystal lattices.[165]

By designing the core-shell fillers with a BN shell whose permittivity is close to that of the matrix for minimized space charge density at the interfaces, Luo et al.[143] added 3 wt% BN-coated $BaTiO_3$ fillers into PVDF matrix. Figure 13 shows that the dielectric strength of the polymer composites containing $BaTiO_3$ micro-hybrid fillers was enhanced by more than 160% of the host PVDF. The electrical current dropped most effectively (10x) when using BN coated BT particles. Internal space charge density between particles and at particle-matrix interfaces is much lower in the same composite design when subject to an electric field in the arrow direction. All these results appear to suggest the importance of incorporating 2D fillers or coatings with high thermal conductivity, such as 2D BN.

3.2.4 | Organic core-shell structure

Organic functionalization as a coupling agent is employed to enhance the interfacial interaction, compatibility, and dispersion of fillers in a polymer matrix. Inorganic dielectric fillers have been modified with organic dielectric materials by chemical treatment, grafting shell layers, using multiple hierarchical shells on the surface of the fillers, or multi-layered structures as reviewed in refs.[166–169] Luo et al.[168] summarized the range of organic modifiers for improving filler dispersion and compatibility with a polymer matrix. Based on this information, the authors tabulated the combination of inorganic core and organic shell in a simpler format, as shown in Table 3.

In essence, an organic functionalization can improve the interface bonding strength between the polymer matrix and inorganic fillers and also the filler dispersion. Scientists carried out chemical treatments through the absorption of coupling agents such as silane, or through

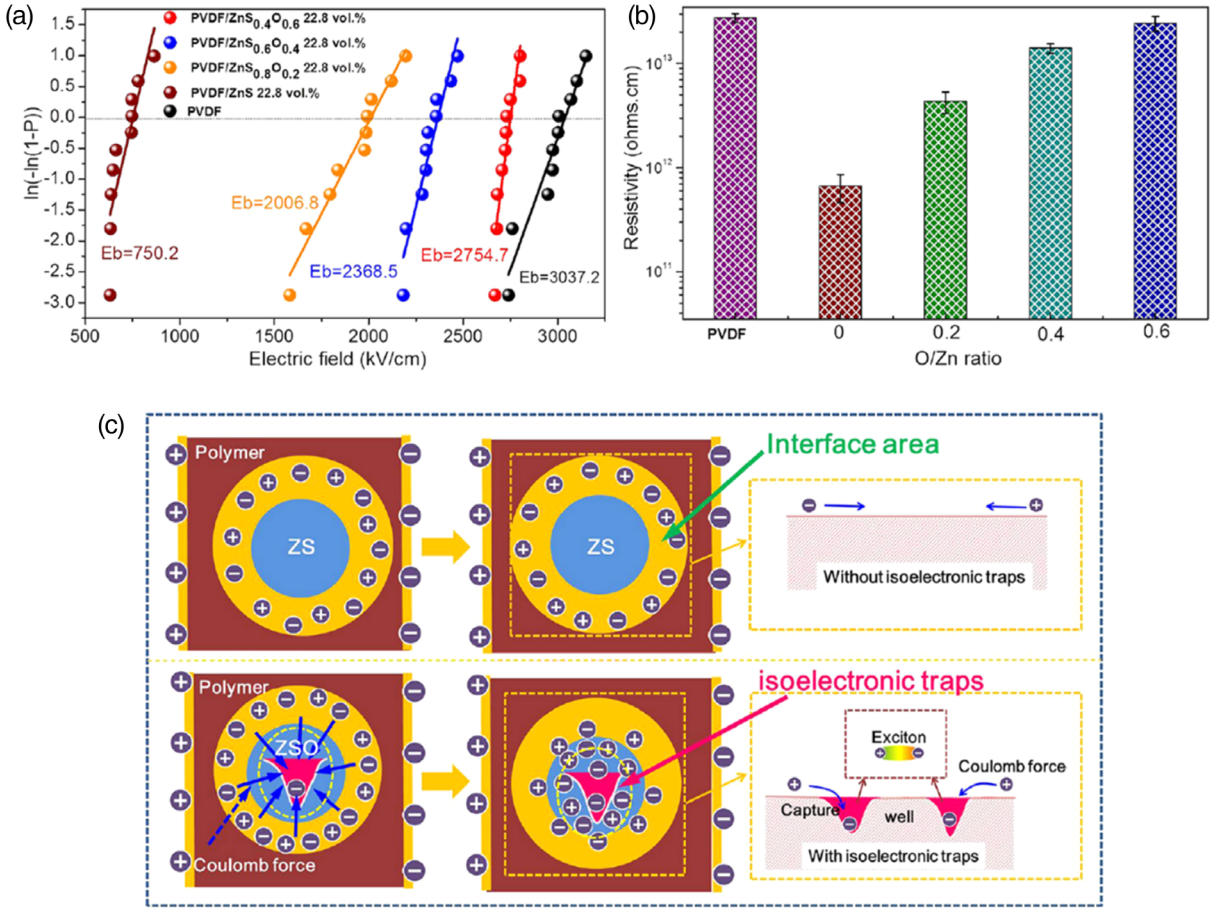

FIGURE 11 (a) Weibull distribution; (b) resistivity values of PVDF/ZSO films with different oxygen contents; (c) Schematic diagram of the mechanism of improved breakdown strength for PVDF-based composites with high filler loading. Reproduced with permission.[142] Copyright © 2019, American Chemical Society [Color figure can be viewed at wileyonlinelibrary.com]

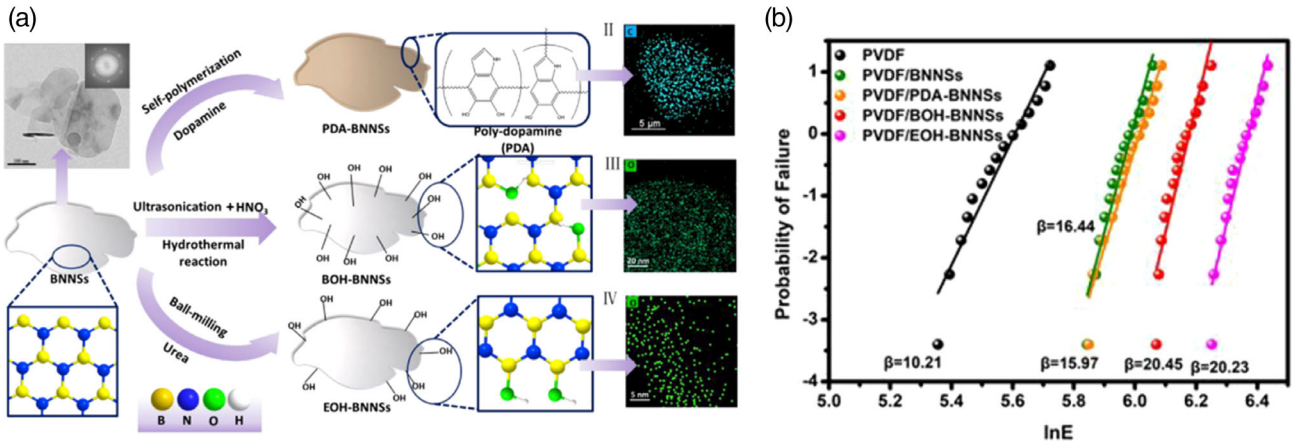

FIGURE 12 (a) The modification process of f-BNNSs and PVDF/BNNSs and PVDF/f-BNNSs nanocomposites films. (b) Weibull plots for PVDF/BNNSs and PVDF/f-BNNSs nanocomposites at the filler content of 10 wt%. Reproduced with permission.[165] Copyright © 2019, The Royal Society of Chemistry [Color figure can be viewed at wileyonlinelibrary.com]

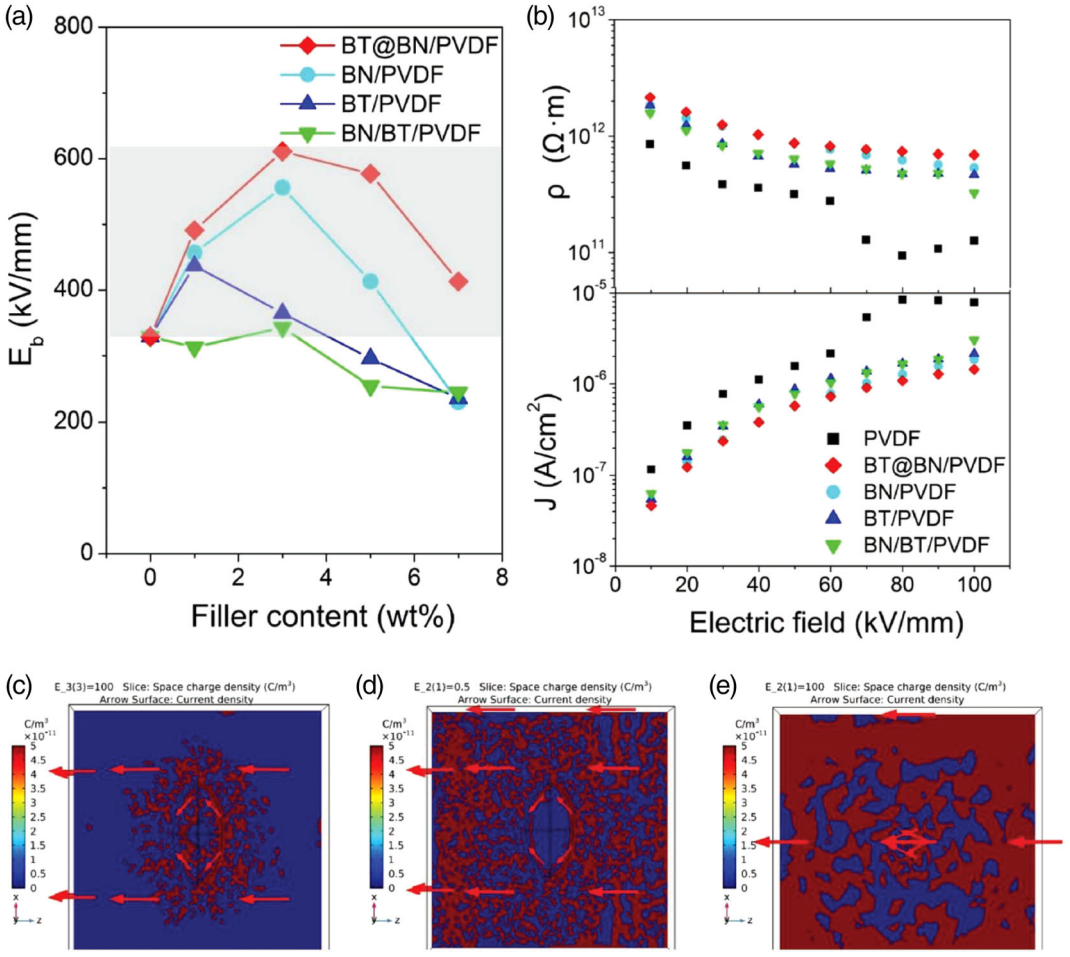

FIGURE 13 Comparison of dielectric strength enhancement of several composite design. (a) Variation of E_b with the filler content of the four types of films; (b) Resistivity and leakage current density as a function of the electric field of the PVDF and the composite films filled with 3 wt% of fillers; (c–e) The simulated space charge density distribution in the PVDF composites filled with BT@BN, BN, and BT, respectively. Reproduced with permission.[143] Copyright © 2019, WILEY-VCH Verlag GmbH & Co. KGaA, Weinheim [Color figure can be viewed at wileyonlinelibrary.com]

TABLE 3 Summary of the range of modifiers used for filler surface modification in dielectric nanocomposites. The filler type and polymer matrix are also indicated based on the study by Luo et al.[168]

Core filler	Dielectric constant	Organic modifier (shell)	Polymer matrix	Process methods	Inorganic shell
Particle	High-K $BaTiO_3$	Phosphonic acid, carboxylic acids, polyvinylprrolidone, dopamine/ polydopamine, hydantoin epoxy, hyperbranched polyamide, poly (trifluoroethyl acrylate)	PVDF base	Surface absorption, grafting, polycon-densation	TiO_2, Al_2O_3, SiO_2, Fe_3O_4, C, Ag
	High-K $BaTiO_3$	PHEMA@PMMA, HBP@PMMA	PMMA base		
	High-K $BaTiO_3$	Gallic acid	PVA		
	High-K $BaTiO_3$	Polystyrene	Polystyrene		
	High-K $BaTiO_3$	Amino-terminated silane molecules	Glycidyl methacrylate		
	Low-K Al_2O_3	Phosphonic acid-terminated poly(ethylene-co-1-butene)	Polypropylene		
	Low-K SiO_2	Fluoride 1H,1H,2H,2Hper-fluorooctyltriethoxy-silane	P(VDF–HFP)		C
Fiber	High-K $BaTiO_3$	Fluoro-polydopamine, PVP	PVDF base	Surface absorption, grafting, polycon-densation	TiO_2, Al_2O_3, SiO_2
	High-K $BaSrTiO_3$	H_2O_2, ethylenediamine	PVDF base		
	High-K $NaNbO_3$	Polydopamine	PVDF base		
Platelet	Graphene	Hyperbranched aromatic polyamide, polydopamine	PVDF base, PBO	Grafting	
	Graphene oxide	PVA, p-phenylenediamine	Nitrile butadiene rubber, polyimide, PVDF-base		
	Boron nitride	g-Aminopropyl triethoxysilane	PVDF		

Abbreviations: PBO, poly(p-phenylene benzobisoxazole); PMMA, poly(methyl methacrylate); PVA, poly(vinyl alcohol; PVDF-base, PVDF, P (VDF–HFP), poly(vinylidene fluoride-trifluoroethylene-chlorofluoroethylene, poly(vinylidene fluoride-trifluoroethylene-chlorotrifluoroethylene; PVP, polyvinylprrolidone.

reactions with metal alkoxides, epoxides, such as propylene oxide, and alkyl or aryl isocyanates.[170] Sabzi et al.[171] carried out the surface treatment of TiO_2 nanoparticles with aminopropyltrimethoxysilane (APS) and investigated its effect on the mechanical and UV-protective properties of a polyurethane composite coating. Tao et al.[172,173] studied the mechanical properties of silane-modified Al_2O_3 nanoparticle filled PMMA composites and found that 5 wt% loading of alumina nanoparticles in PMMA caused an increase in strain-to-failure of over 28%, which enabled plastic flow in the glassy state. Dopamine has been used as the surface modifier for various fillers due to its adhesive properties.[174] For example, $BaTiO_3$ nanofibers modified with dopamine of ~5 nm thick layer resulted in an increase in relative permittivity by ~20% and breakdown strength by ~100% compared to an epoxy composite control.[175] $BaTiO_3$ nanoparticles were chemically treated by titanate coupling agent which is very useful for enhancing the breakdown strength and energy density in PVDF composite and may be useful in other inorganic-polymer systems.[176]

Scientists improved the dispersion of monodisperse and spherical TiO_2 nanoparticles by optimizing the oxygen flow rates in the gas-aggregation chamber and coating with uniform paraffin nanoshells (>13 nm) as they were *in-flight* toward the substrates. The paraffin containing core-shell nanoparticles also show higher dielectric constant and lower dielectric loss with respect to bulk paraffin; however no dielectric strength improvement exhibited.[177] Titanium dioxide nanoparticles capped with oleic acid OA-TiO_2 were solution-processed to form homogeneous dielectrics for organic thin-film transistors, TFTs with top-gate and bottom-gate

configurations.[178] This suggests a promising high-K dielectric with low leakage current for organic TFTs.

Working with multicomponent composites, scientists have developed several models in predicting the dielectric constant of the composites, which include Maxwell-Wagner model, Logarithmic Mixing Law and Bruggeman Model. These models describe composites based on the respective dielectric constant of the polymer, inorganic filler, composition ratio as well as the filler sizes. A better model introduced an interphase interaction factor ($K_{interface}$) and its contribution to the composite dielectric constant, as shown in Figure 14a.[179,180] A strong filler/polymer interaction (positive large $K_{interface}$ factor) increases the effective dielectric constant of composites when the filler has a higher dielectric constant than the polymer matrix. As such, a stronger interaction or bonding between the two participating dielectric materials is desirable for a high dielectric constant. For a core-shell design, a polymer composite having a stronger interface should also be preferable for suppressed charge mobility, electrical conductivity, and improved dielectric strength. An example of the slimmer polarization loop of the composites embedded with strongly bonded filler-polymer is shown in Figure 14b. The improvement may be understood as such an interface renders fewer interfacial defects for charge initiation.[181]

For organic species with only physical absorption, the weaker bonding and free residual species in the composites results in a high leakage current and dielectric loss. The issue can be avoided by forming covalent bonding between the organic modifier and core particles. Many investigations have utilized a grafting approach.[182–184] A PVDF nanocomposite with embedded PVP-encapsulated gold (Au) nanoparticles exhibits enhanced nanoparticle dispersion due to the favorable particle-polymer interaction.[185] The surface functionalization of Au nanoparticles, however, failed to reach low dielectric loss and high dielectric strength. An insulating fluoropolymer having similar chemical structure and surface energy to P(VDF-HFP) matrix was coated on BT via surface-initiated reversible addition−fragmentation chain transfer (RAFT) polymerization. This process enhanced the dispersion of BT nanoparticles and interfacial adhesion, as shown in Figure 15. The nanocomposites with a thick fluoropolymer shell exhibited a lower dielectric loss, bigger polarization loop and enhanced energy storage capability in comparison with the pure P(VDF–HFP); for example, 6.23 J cm^3 for a nanocomposite with 50% $BaTiO_3$–PTFEA2 and 4.10 J cm^3 for P(VDF–HFP). The

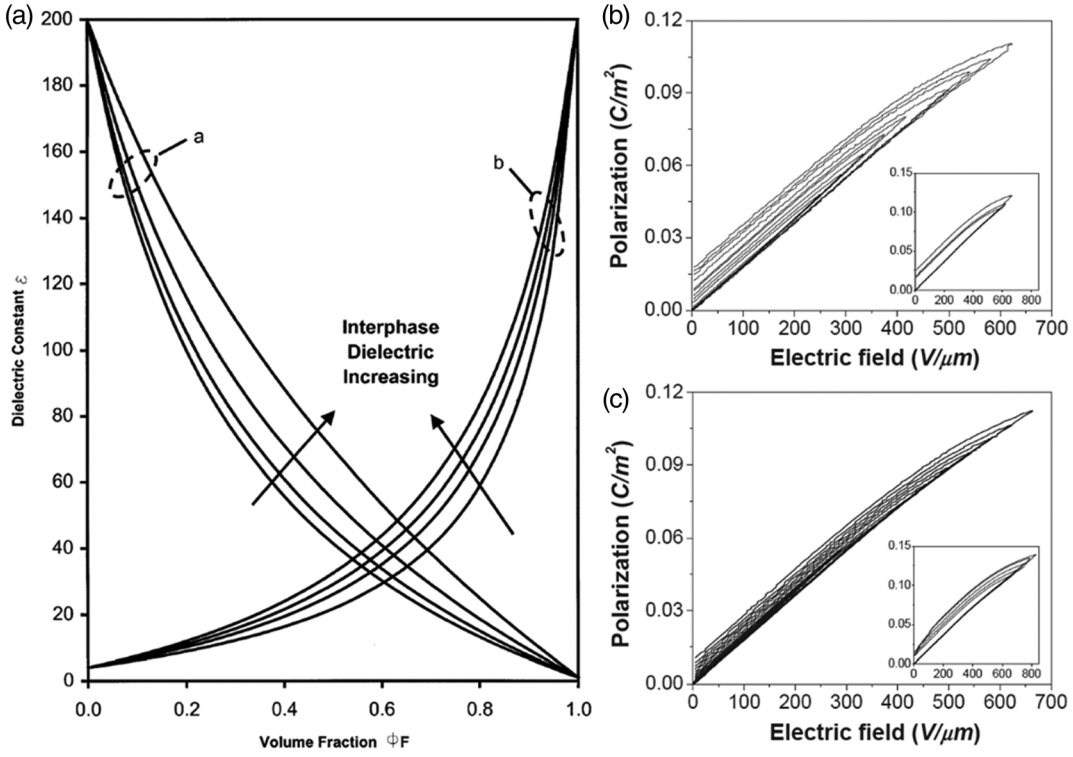

FIGURE 14 (a) The prediction of the dielectric constant of composites as a function of filler fraction for different values of $K_{interface}$. a for the case of $K_{filler} < K_{polymer}$ and b for $K_{filler} > K_{polymer}$; Reproduced with permission.[179] Copyright © 2002, Elsevier. (b,c) Field-dependent polarization loops for neat CNETMS and CNETMS/OPA-SAM bilayer films. Polarization hysteresis loops above the field strength of 600 V /μm are shown in the inset. Reproduced with permission.[180] Copyright © 2015, WILEY-VCH Verlag GmbH & Co. KGaA, Weinheim

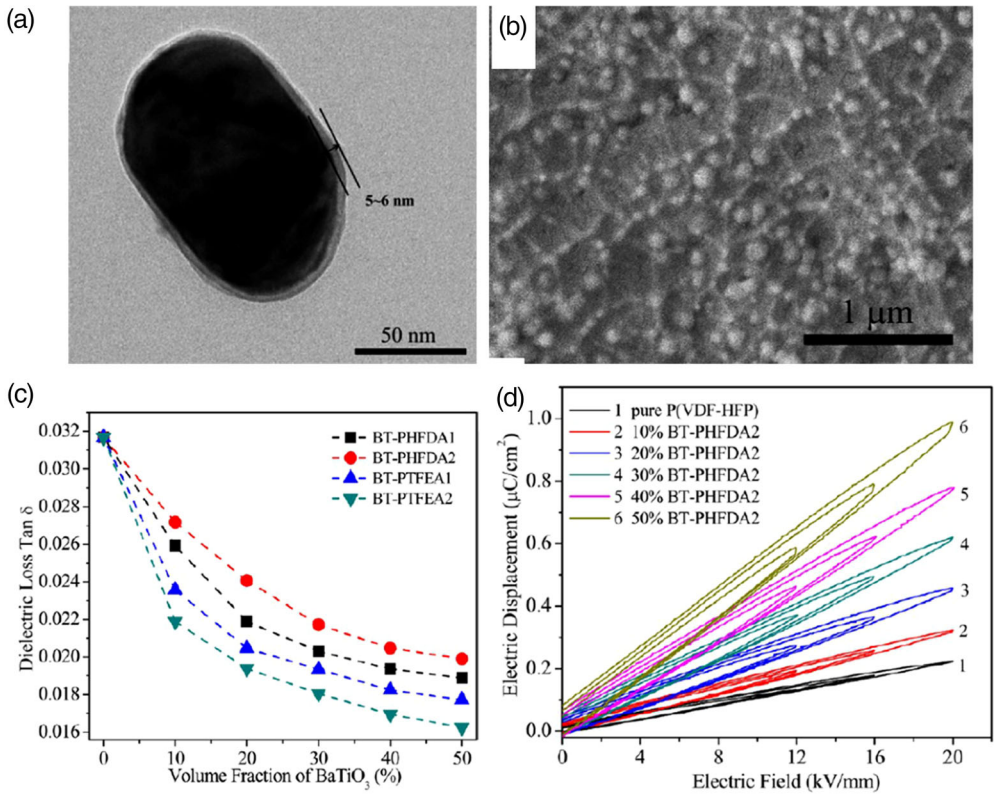

FIGURE 15 (a)TEM image of fluoro-polymer@BT nanoparticles BT-PHFDA2 (Figure 3b), (b) SEM images of the freeze-fractured cross sections of fluoro-polymer@BT and P(VDF-HFP) nanocomposite films with 20 vol% of BT nanoparticles BT-PHFDA2 (Figure 4b); (c) Dielectric loss of P(VDF-HFP) with BT-PHFDA1, BT-PHFDA2, BT-PTFEA1, and BT-PTFEA2 at 1 kHz. (Figure 8b). (d) Electric displacement-electric field (*D-E*) loops of the P(VDF-HFP) with nanoparticles BT-PHFDA2 (Figure 9b) Reproduced with permission.[186,189] Copyright © 2013, American Chemical Society [Color figure can be viewed at wileyonlinelibrary.com]

limited decrease in dielectric loss and increase in dielectric constant may be due to the upward shift of crystallization temperature with the addition of fillers and stronger interfacial bond.[186] However, fluoropolymer (e.g., PVDF, PTFE, ETFE) having very low surface energy requires careful selection of chemical modifiers to avoid undesirable dielectric properties. Adoption of the fluorine atoms for modifier shell can form stronger hydrogen bonds with hydrogen atoms between modifiers and polymer matrix. This method results in higher dielectric constant and lower dielectric loss; however, no improvement in dielectric strength.[187]

Grafting of synthetic polymers to the inorganic filler surface not only enhances the chemical functionality, but also alters the surface topology of the natural inorganic materials. Several researchers carried out this route attempting property improvement. They developed small molecule ligands or polymer brushes using a polyhedral oligomeric silsesquioxane (POSS) ligand containing seven isobutyl and two phosphonic acid groups, POSS(PA)2. The choice of two adjacent phosphonic acid groups is to enhance the conjugation and interfacial bonding strength.[188] It was noticed that grafting fillers with modifiers of different dielectric properties resulted in inconsistent dielectric properties. Poly(dopamine) (PDA) encapsulated $BaTiO_3$ nanoparticles (PDA@BT) were added to a PVDF matrix cross-linked by a free radical initiator. PDA coating results in a more homogeneous dispersion in the matrix. The formation of hydrogen-bonding between the PDA layer and the polymer, especially the chemical cross-linking across the matrix, resulted in improved breakdown strength by ~40%, and decreased conductivity by nearly 1 order of magnitude when compared to BT filled composites. However, the dielectric loss is higher than in the neat polymer matrix, and the dielectric strength of the neat polymer reference is quite low.[189,190]

Better nanoparticle separation and interfacial structure were achievable using hairy nanoparticles, as shown in Figure 16. The US AFRL[191,192] grafted polystyrene matrix polymers to nanoparticle surfaces and observed significant benefits in maintaining dielectric breakdown strength and improving dielectric loss for $BaTiO_3$ and TiO_2-based nanocomposites. However, the dielectric strength of the composite is not better than the neat polymer itself across all loading fractions of fillers. Still, these findings revealed the advantages of high molecular weight polymer for functionalizing the nanoparticles polymer-based nanodielectric composites.

The effect of interfacial layer thickness was further investigated using a rigid liquid-crystalline polymer PMPCS as a modifier for $Na_2Ti_3O_7$ NFs by RAFT in situ polymerization. The nanocomposite showed significantly increased permittivity due to the increased thicknesses of PMPCS shell. The improvement of dielectric strength remains to be achieved.[193] Fluoric-liquid-crystalline

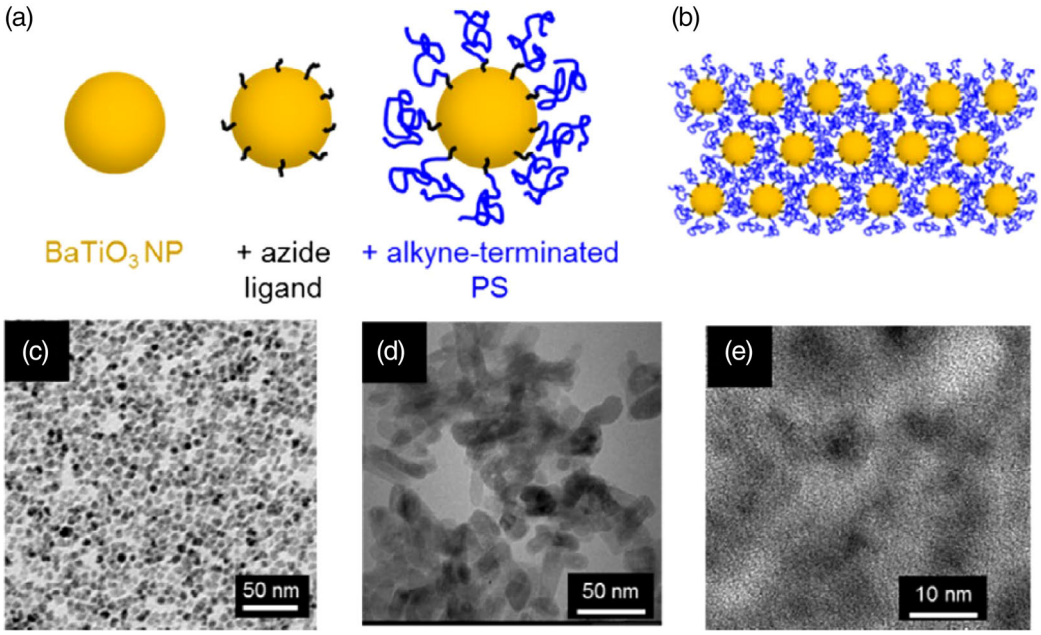

FIGURE 16 (a) Overview of HNP "click" chemistry synthesis; nanoparticles are functionalized with azide ligands that facilitate grafting of alkyne-terminated polystyrene chains. (b) Illustration of ideal assembled hairy nanoparticle film. TEM images of (c) bare $BaTiO_3$ and (d) TiO_2 nanoparticles. (e) Representative TEM of 22% v/v HNP PS@$BaTiO_3$, demonstrating evidence of fractal-like structure.[191] This is an Open Access article permitting unrestricted use [Color figure can be viewed at wileyonlinelibrary.com]

polymer PFTMPCS were also designed and synthesized to tailor the surface of $BaTiO_3$ nanowires and nanoparticles via the RAFT polymerization method. A high discharge energy density of 14.64 J/cm^3 was obtained due to the combination of a high polarization with high breakdown strength of the nanocomposites.[184,194] The energy efficiency decreased from 93.64 to 56.64% as the BT loading increased from 0 to 50 vol%, which is related to the enlarged P-E loop. This novel approach may provide an inspiring path for various nanostructured materials; however appropriate organic modifiers and chemical reaction processes may prevent the contributions of interfacial polarization and residual mobile organic species.

Li et al.[118] attempted the combined effects of inorganic shell and organic grafting. They coated a Al_2O_3 layer of intermediate permittivity on high-permittivity $BaTiO_3$ as a buffer layer between the nanofiller and the polyolefin matrix. Chemisorptive activation of the single-site metallocene catalyst [rac-ethylenebisindenyl] zirconium dichloride ($EBIZrCl_2$) was enabled on the inorganic core-shell fillers by in-situ polymerization to disrupt nanoparticle agglomeration. Tuning the thickness of the Al_2O_3 coating has little effect on the nanocomposite permittivity, but dramatically lowers the leakage current and dielectric loss. Unfortunately, this early endeavor to tackle the disruptive issue at the filler-polymer interface did not report dielectric breakdown withstanding capability. Additional investigations ought to be carried out.

3.3 | Coating film surfaces

Dielectric strength as an intrinsic material property is sensitive to the interior nature of the material and its surface condition. The latter is more closely determined by material processing, especially in its thinning process. Minimizing the surface defects and contamination and their adverse contributions becomes more critical for polymer films thinner than 10 μm, which are desirable for compact capacitor technology. A conventional approach is to deposit a layer of organic material on the surface of a polymer film to reduce the nonuniformity of the film surface and the adverse effects of surface defects. Yializis patented this concept that could improve the dielectric strength of dielectric polymer films.[195] The organic coating concept are applicable to multilayer lamination, and more details are available elsewhere.[24] However, this organic coating method has not been widely used partially because of its poor performance. An inorganic oxide coating has been well known as a gas barrier for polymer films, but its effect on dielectric strength was investigated only 10 years ago.

The author conducted this type of coating research using various polymer film substrates (e.g., PEI, CN-PEI,

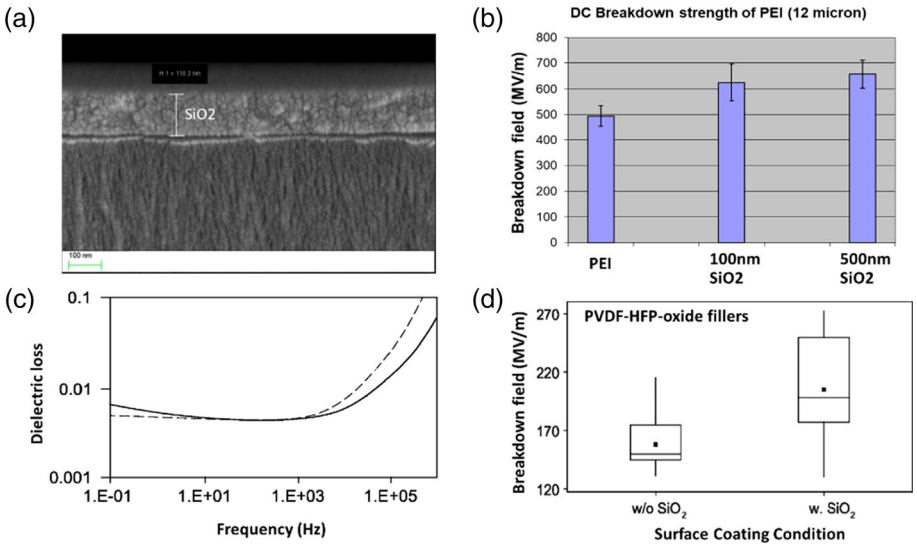

FIGURE 17 (a) SEM image of SiO_2 coating on 12 μm thick PEI; (b) Comparison of DC dielectric strength between neat film and films coated with different SiO_2 thicknesses; (c) Dielectric loss as a function of frequency of measurement of 100 nm SiO_2 coated PEI film; (d) A box plot comparison of breakdown strengths of a polymer composite PVDF-HFP with and without SiO_2 coating.[196,197] [Color figure can be viewed at wileyonlinelibrary.com]

PC, PI, and PVDF) at General Electric Company for high temperature and high energy density capacitor technology.[196,197] The inorganic coating on them all has a positive effect on enhancing the dielectric strength of the underlying films. Figure 17 shows the example of SiO_2 coating on a polymer film and the corresponding dielectric properties. Similar improvement exhibited in cyano-modified PEI, PC, and PP films. The inorganic coating materials can be silicon oxide, aluminum oxide, titanium oxide, tantalum oxide, strontium titanate, SiNx, etc. The conformal coating can be deposited in the thickness range of 25–500 nm, as shown in Figure 17a. Apparently, up to 30% increase in DC dielectric strength was achievable for both pure PEI film and PVDF-HFP (polyvinylidenedifluoride-hexafluoropropylene) composite films containing oxide fillers as shown in Figure 17b,d without causing much increase in dielectric loss.

Various coating methods show feasibility and efficiency. Among different deposition techniques (sputtering, reactive sputtering, PECVD, e-beam, and ALD), e-beam turns out to be the fastest one for nanometer layers.[38,198] Inorganic coating techniques were also adopted by other research laboratories, including, but not limited to, Penn State University, RPI, UT Austin, MIT, Tsinghua University, Beijing Institute of Printing, etc.[199–204] For example, the resulting Si_3N_4/P(VDF-CTFE) bilayer film exhibits significantly reduced conduction loss over a single layer of P(VDF-CTFE), while maintaining a high energy density. BN coating on polymers like PEI, BOPP, FPE, PI, and c-BCB resulted in higher dielectric strength for a given charge–discharge efficiency at above 100°C. Recent work further demonstrated that the enhancement of dielectric strength becomes more apparent at higher temperature when coating with higher thermal conductivity *h*-BN.[204] For a charge–discharge efficiency, this increase can be in the range of 30–100% for PEI and other high-temperature polymer films at temperatures >125°C, as shown in Figure 18.

The interfacial role between two different dielectric materials has been well recognized and also utilized for multilayer design between polymers.[180] As previously mentioned in Figure 13b, a bilayer structure was deposited using a hybrid sol–gel dielectric of 2-cyanoethyltrimethoxysilane (CNETMS) and an n-alkylphosphonic acid (PA-SAM) layer. The PA-SAM between the sol–gel film and the metal electrode serves as a charge-blocking layer to suppress carrier injection from an aluminum metal electrode into the sol–gel film that mitigates associated electrical conduction in the sol–gel films at high electric fields. The CNETMS/PA-SAM bilayer structure shows outstanding improvements in electrical failure reliability, energy extraction efficiency (72%), and energy storage density (40 J/cm^3), as compared with previously reported capacitor devices.

The interface concept was also applicable to polymer-based nanocomposite films. A (P(VDF–HFP) template polymer was used to construct a sandwich-structured composite. It consists of a pure poly(vinylidene fluoride-co-hexafluoropropylene (P(VDF–HFP)) central layer and $BaTiO_3$/P(VDF–HFP) upper and lower layers using a spin-coating process.[205–207] However, this type of sandwich-structured composite often suffers from a low relative permittivity, and polarization due to the central polymer layer having low permittivity, and also process complexity for scale-up.

Nanolaminated polymer films consisting of multilayer nanoscale layers are one type of the all-polymer composites by co-extrusion of two or more polymer resins. It is reliable to improve dielectric strength of polymer

composite films this way in terms of physical principles. Laminating hundreds of nanometer layers of dissimilar polymers has been proven to be feasible in a university laboratory (Figure 19).[25,208–211] Multilayer film technology is of particular interest because one can design the multilayer films using alternating layers of a high-K polymer and a linear dielectric polymer with low dielectric loss and high breakdown strength. The unique one-dimensional system with tailored material choices and interfaces may minimize the disadvantageous polarizations and maximize the dielectric strength for future polymer film capacitors. In comparison with blend

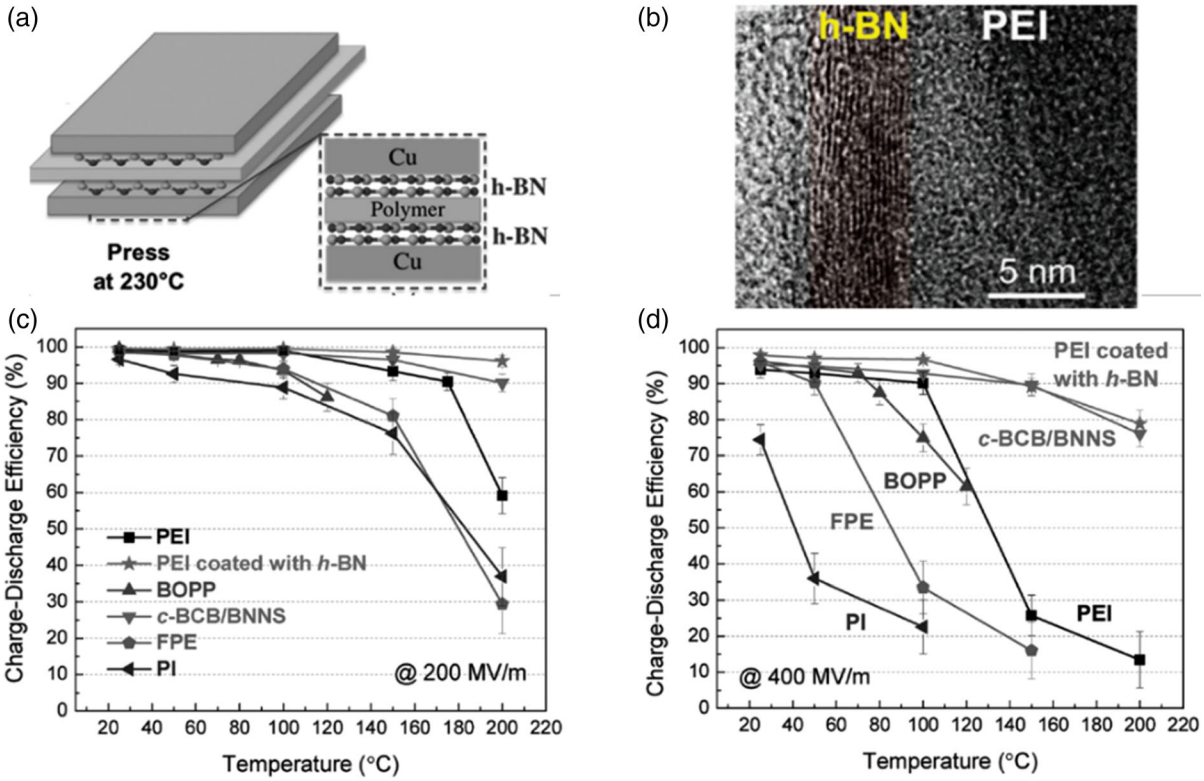

FIGURE 18 (a) Schematic of the CVD-grown *h*-BN films on Cu electrode sandwiching the polymer films; (b) Cross-sectional HRTEM image of the microtomed slice of the sandwich-structured film, confirming the presence of the *h*-BN film on the surface of PEI; (c) Charge–discharge efficiency of the dielectrics as a function of temperatures measured at an applied field of 200 MV/m; and (d) 400 MV/m. Reproduced with permission.[204,209] Copyright © 2017, WILEY-VCH Verlag GmbH & Co. KGaA, Weinheim [Color figure can be viewed at wileyonlinelibrary.com]

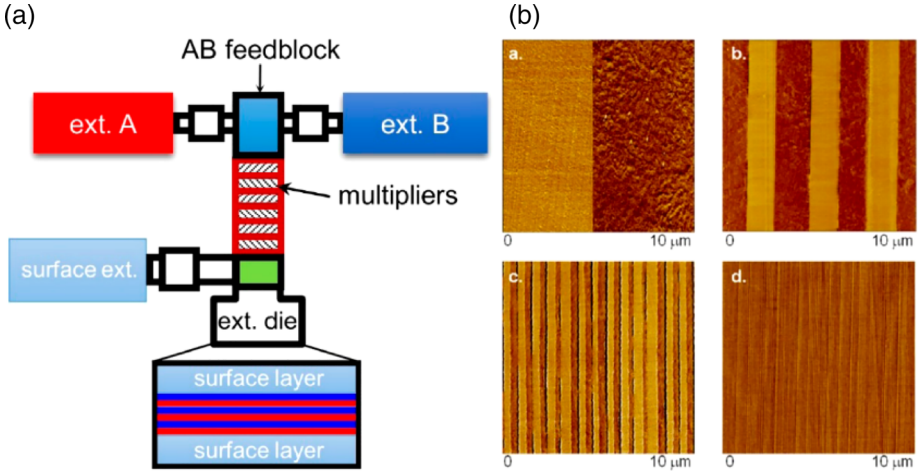

FIGURE 19 (a) Schematic representation of the multilayer coextrusion process. (b) AFM phase images of PC/PVDF 50/50 (vol/vol) multilayer films: (a) 2-layer, (b) 8-layer, (c) 32-layer, and (d) 256-layer. The total film thicknesses are around 12 μm. The individual layer thicknesses are 6,000, 1,500, 380, and 50 nm, respectively. Reproduced with permission.[25,209] Copyright © 2012, American Chemical Society [Color figure can be viewed at wileyonlinelibrary.com]

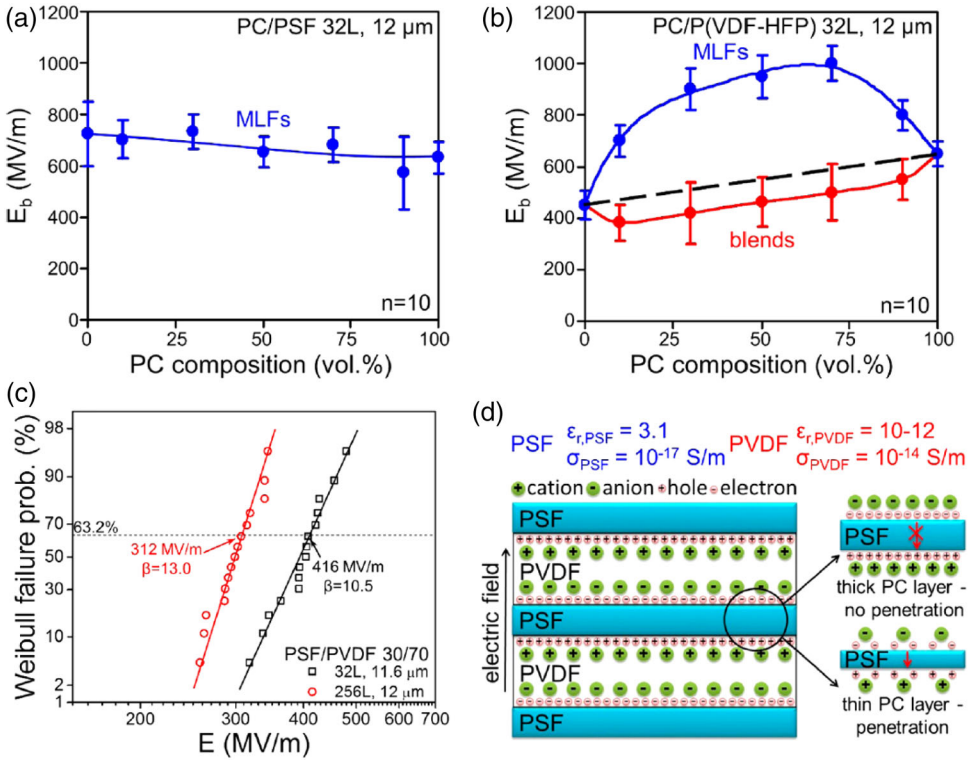

FIGURE 20 Dielectric breakdown strength as a function of PC composition for (a) the PC/PSF 32 L and (b) the PC/P (VDF-HFP) 32 L films measured by the needle-plane method at room temperature. Each data point is an average of at least 10 samples. (c) Weibull analysis of dielectric breakdown strength for the PSF/PVDF 30/70 32 L and 256 L films measured by the plane −plane method (electrode area = 1.77 cm^2) at room temperature. (d) Schematic of the interfacial polarization from both impurity ions and free electrons for the PSF/PVDF multilayer films with either thick or thin PSF layers. Reproduced with permission.[25] Copyright © 2017, American Chemical Society [Color figure can be viewed at wileyonlinelibrary.com]

polymer films, melt-extruded PC/P(VDF-HFP) exhibits higher dielectric insulation, which is attributed to the flat interfaces positioned perpendicular to the applied field direction. However, the breakdown strength of the multiplayer composites may present no improvement or lower values when the composing polymer is not adequately selected as shown in Figure 20.[25] Certain interfacial electrons may be introduced through the poorly insulated polymer responsible for the consequences. Therefore, it is necessary to develop viable strategies for the compatible polymer combination with reduced interfacial defects for practical large-scale film applications and large test electrode fixtures.

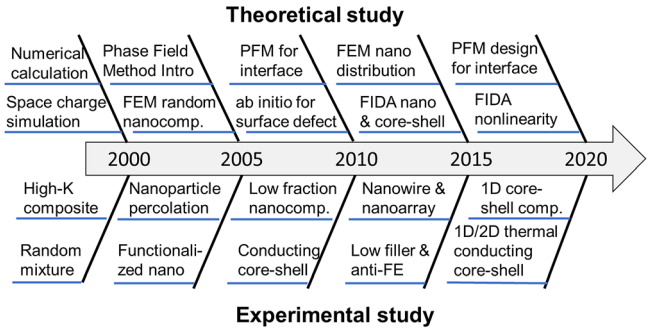

FIGURE 21 Progressive efforts in dielectric materials investigation [Color figure can be viewed at wileyonlinelibrary.com]

4 | DISCUSSION OF MECHANISMS OF DIELECTRIC ENHANCEMENT

Adding nanometer fillers into a polymer not only incorporates the nature of the fillers themselves, but also generates multiple interfaces (the third phase), which together change the properties of the hosting polymer. Gradually, the dielectric community recognized the importance of interfaces; however understood less about how they contribute and when they become critical to dielectric strength. The review of the above publications once again illustrates the progressive efforts made toward dielectric strength improvement using various fillers, polymers, processes, and testing techniques. The explanation of those results and mechanisms of the fillers and interfaces in nanodielectrics is far from being satisfactory. Nevertheless, based on the prior published work, one can trace an investigation pathway toward the enhancement of dielectric strength, as described below. Figure 21 shows a progressive improvement being made using various technical approaches over the years. Both experimental and theoretical efforts dealt with nanoparticle synthesis, functionalization, nanodielectric composite processing, and polymer film improvement. After the initial perplex playing with nanofillers, the dielectric community came up with a rational design strategy reducing innovations to practice. By combining low-dimensional fillers and

core-shell structures, more than 50% increase in dielectric strength was achievable. Leveraging thermal conducting materials provided a new horizon to the challenging problem. Considering the complications in various hypotheses, models, and mechanisms for dielectric breakdown, the author makes some general comments on the relevant topics in the following. The author also specifically pointed out the possible combined effect of thermal conduction and electric breakdown mechanism.

4.1 | Dielectric breakdown mechanism for thin films

Some degradation happens inside the bulk material, and some initiates at the surface of dielectric films usually thinner than 100 μm. A deeper understanding of the breakdown mechanism has been obtained from very thin oxide dielectrics and should be discussed here. Since insulators have inherently low conductivities on the order of $10^{-20} \sim 10^{-8}\ \Omega^{-1}\ \mathrm{cm}^{-1}$. Conduction current through the dielectric film is only noticeable when applying a high electric field. Chiu[212] categorized the mechanisms in thin dielectric films into two types of conduction mechanisms, electrode-limited and bulk-limited. (Figure 22a) The most crucial parameter in the electrode-limited conduction mechanisms is the barrier height at the electrode dielectric interface, whereas the most critical parameter in the bulk-limited conduction mechanisms is the trap energy level inside dielectric films. The electrode-limited conduction mechanisms include (a) Schottky or thermionic emission, (b) Fowler-Nordheim tunneling, (c) direct tunneling, and (d) thermionic-field emission. The current due to thermionic emission is highly dependent on the temperature, whereas the tunneling current is nearly temperature independent (Figure 22b). Aside from the electrode-dielectric interface height, the effective mass of the

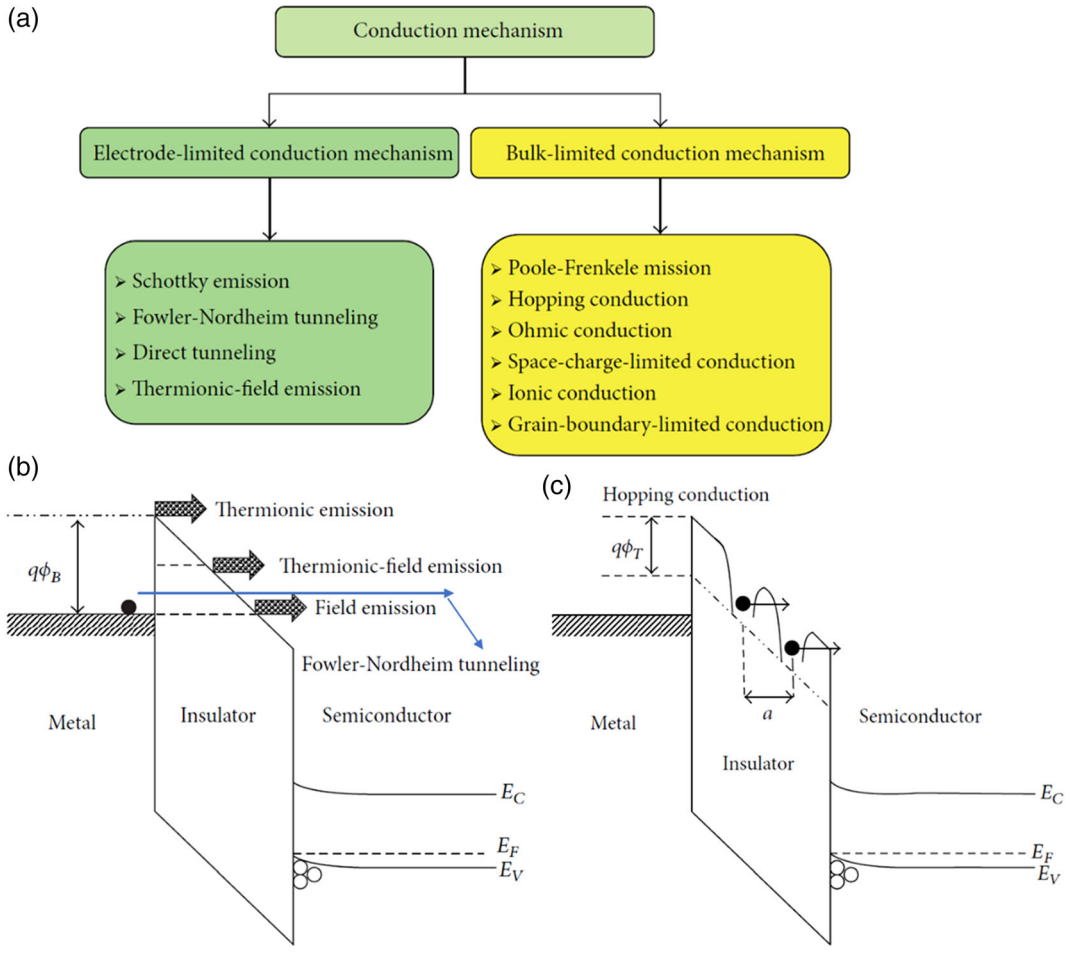

FIGURE 22 Classification of conduction mechanisms in dielectric films (a), Schematic energy band diagram of emission and Fowler-Nordheim tunneling in metal–insulator–semiconductor structure (b), and hopping conduction mechanism (c).[212] This is an open access article permitting unrestricted use [Color figure can be viewed at wileyonlinelibrary.com]

conduction carriers in dielectric films is also essential. The most critical parameter in bulk-limited conduction mechanisms is the trap energy level in the dielectric films. The bulk-limited conduction mechanisms include (a) Poole-Frenkel emission, (b) hopping conduction, (c) ohmic conduction, (d) space charge-limited conduction, (e) ionic conduction, and (f) grain-boundary-limited conduction. Since Poole-Frenkel emission results from the thermal activation under an electric field, this conduction mechanism often works at high temperature and high electric field. Hopping conduction is due to the tunneling effect of trapped electrons "hopping" from one trap site to another in dielectric films as shown in Figure 22c. The trap energy level changes with increasing temperature.

For thin oxide films, Solomon reviewed their breakdown mechanism and explained that the intrinsic breakdown phenomenon is current limited and is described by the Fowler-Nordheim tunneling mechanism.[213] Since the high-field intrinsic breakdown mechanism is mainly process independent, they believe that impact ionization and positive charge accumulation in high-quality SiO_2 thin films below 150 nm can best describe the mechanism. Lombardo et al.[214] also discussed the physics of dielectric breakdown in gate oxides and oxynitrides of thicknesses between about 1 and 35 nm under constant-voltage stress in conditions of direct or Fowler-Nordheim tunneling. These breakdown mechanisms acquired from thin-film oxides may shed some light on the ongoing efforts on thin oxide coating and core-shell particle interfacial junctions.

For most dielectric polymer and nanodielectric materials, the breakdown depends on time, temperature, thickness, processing of materials, defects, fillers, filler-polymer interfaces, and electrode materials. Though many breakdown theories are out there, it is still challenging to decide which mechanism plays a dominant role in the breakdown phenomena. Li et al.[91] emphasized the importance of investigating the multi-hierarchical structure and the macroscopic properties of nanodielectrics to understand the impact of filler and matrix on short-term breakdown and long-term failure separately. It appears that nanoparticles, adequately mixed and dispersed in the polymer matrix, act as barriers obstructing electrical tree growth and delaying dielectric breakdown for long-term endurance breakdown events.[215] For thin dielectric materials and short breakdown events, breakdown mechanisms are more or less related to charge injection, trapping, tunneling, conduction, and thermal runaway at higher field and temperatures. As far as which model and mechanism predominate the dielectric breakdown phenomena in different materials and configurations, it requires more investigation and analysis case by case.

4.2 | Interfaces against electrical charge transport

Since the beginning, filler surface functionalization has become an essential topic as they may cause weak bonding with polymers, a poor filler dispersion (agglomeration), and electrical charge accumulation. However, the organic surface treatment of the nanoparticles is not a necessary premise for enhancing dielectric strength. The inorganic shell design makes a positive impact on dielectric strength and other properties according to the prior publications. This means that the interfacial region between fillers and the polymer matrix plays a critical role. It is the same case for a film surface, where the interface occurs between a film and electrodes or coating layers. In both cases, the enhancement in dielectric strength repeatedly occurred. Therefore, understanding the role of interfaces and the mechanism is quite pressing.

Currently, the roles of interfaces reside in their function as charge transport barrier and charge traps. In the former case, the interface comprises an inorganic shell or surface coating, which raises the energy barrier height and blocks the charge injection and movement. Prior experiments on *h*-BN-coated PEI films also showed increased electrical resistivity and energy barrier charges demonstrating more difficulty for the electrons to be injected into the samples. The suppression and delay of charge transport lead to a higher energized voltage. In the latter case, the interface is composed of conductive fillers and surrounding insulating polymers or shell material, which become localized field sites attracting charges. The electrons and holes being directed to these places by a high electric field may eventually tunnel through or hop around to conduct current unless the sites are limited and isolated by great distances. When the interface dielectrics are very thin (nm), Fowler-Nordheim tunneling may be the dominant mechanism, and higher breakdown strength and low dielectric loss may result. When dielectric films are exposed to high electric fields and temperatures, a hopping mechanism may play a role by releasing the trapped charges and causing higher electrical conductivity and failure.[87] Phase-field modeling is a useful tool and can be well utilized to study the dielectric breakdown phenomenon of polymer nanocomposites.

4.3 | Intrinsic thermal conduction

The reported greater enhancement in the dielectric strength of nano-filled composites is mostly associated with dielectric materials with high thermal conductivity. A good example is the involvement of BN platelets or BN

coatings.[216] It is known that charge carriers transport not only electrical current, but also heat. The fast dissipation of thermal energy through shells or fillers is favorable for the extension of failure to higher voltages. High thermal conductive fillers can transport the heat out more effectively so that the local temperature rise induced by the localized electric field around the fillers is minimal, and thus the local regions maintain a higher voltage withstanding capability. Thermally conductive fillers such as BBNS with an insulating shell (polydopamine) even further improve the interfacial compatibility between the two phases and thus higher dielectric strength.[217] This is true for voltage endurance to be enhanced using mica tape containing BN fillers for generator and motor insulation.[218,219] Recent computer simulation based on an electrothermal breakdown phase-field model also reveals the mitigation of heat-induced deterioration of dielectric strength through high thermal conductivity BNNS in film capacitor construction (Figure 23).[220] The simulation suggests that reducing the electrical conductivity is more effective in comparison with enhancing the thermal conductivity as the reduced electrical conductivity of the polymer nanocomposites reduces the thermal effects. The authors summarized the connection of dielectric strength improvement with the thermal conductivity of fillers being used in polymer composites, as shown in Figure 24a. The commonly used fillers with low thermal conductivity generally result in less improvement when using no core-shell or low-dimension filler. The fillers with very high thermal conductivity result in a good record of bigger improvement. AlN is another example supporting the improved dielectric strength compared with other low thermally conductive oxides in the literature.[221,222] It appears that the existence of electrically conductive fillers may also benefit from the heat dissipation because of their high thermal conductivity. The investigation of the synergy between thermal conduction and electric breakdown in polymer composites may become a meaningful approach toward enhanced breakdown strength and understanding of the dielectric breakdown mechanism.

4.4 | Lower dielectric strength in baseline samples

Dielectric strength closely depends on the destructive tests that are sensitive to sample processing, test methods, operators, besides the dimension, composition, structural ordering, crystallinity, and test conditions, etc. Some improvements in dielectric strength in composites may not be genuine, but rather the result of lower values in the pure polymer baselines to which they were compared. For example, VDF-containing polymers have over 50 different grades, and researchers use different compositions and copolymer chemistry that are difficult to know. In the various publications, the DC dielectric strength of PVDF films is in the broad range of 300–600

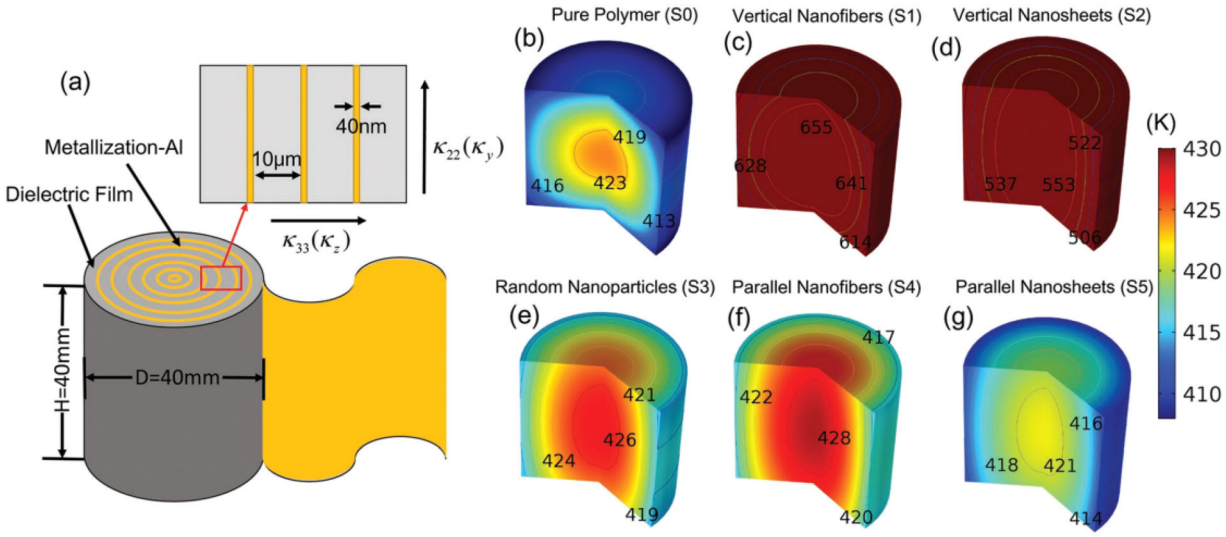

FIGURE 23 (a) Schematic illustration of a real capacitor with a height of H = 40 mm and a diameter of D = 40 mm, made by winding the PI-STO nanocomposite film. When working under an applied electric field of 200 kV mm − 1 and a surrounding temperature of 400 K, the steady-state temperature distributions in different capacitors made by film nanocomposites filled by (b) pure polymer S0, (c) vertical nanofibers S1, (d) vertical nanosheets S2, (e) random nanoparticles S3, (f) parallel nanofibers S4, and (g) parallel nanosheets S5. Reproduced with permission.[220,227] Copyright © 2018 WILEY-VCH Verlag GmbH & Co. KGaA, Weinheim [Color figure can be viewed at wileyonlinelibrary.com]

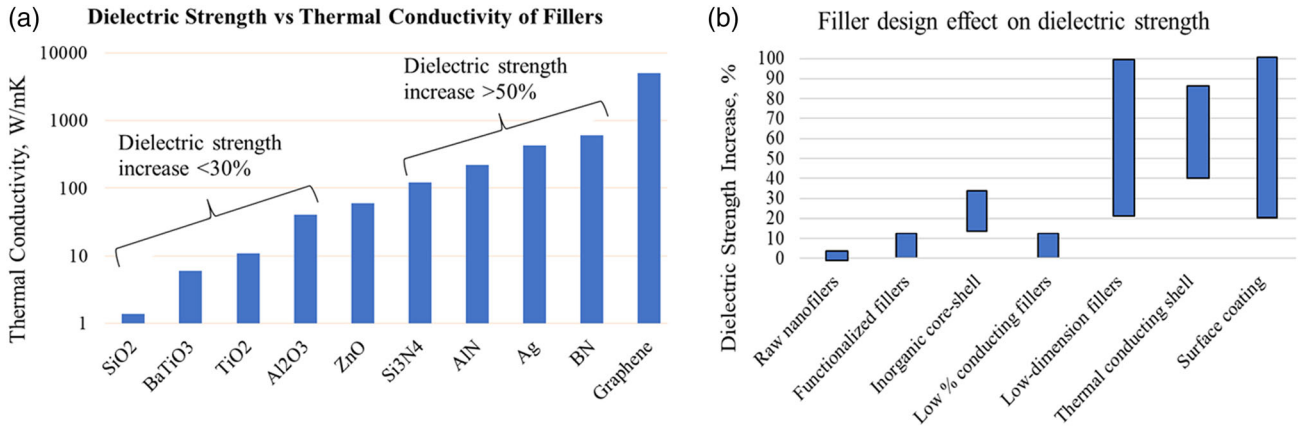

FIGURE 24 (a) The relationship between the thermal conductivity of fillers and the dielectric strength improvement. (b) Effect of various technical routes on dielectric strength improvement of polymer dielectrics [Color figure can be viewed at wileyonlinelibrary.com]

MV/m. The values are even higher for the uniaxially oriented film (>600), and biaxially oriented film (>700).[223,224] In fact, most of the increased dielectric strength with respect to their baseline claimed in the publications is below 600 MV/m, surely lower than that of biaxially oriented PVDF. Taking epoxy as another example, its DC dielectric strength is in the range of 35–170 MV/m.[225] A good epoxy sample can have quite high dielectric strength. In some of the progress reports, baseline values were very low, thus, the increases in dielectric strength were claimed in filled composites. Nevertheless, the increased values remain in the previous dielectric strength range for the pure polymers.

It is fair to ask the question: are some of the enhancement claims due to the lower baseline values or increases in the composites? It would be more rigorous to pay more attention to the baseline sample preparation and characterization while claiming a particular increase in nanofilled polymer composites. It is the author's view that one may not need a very high enhancement in dielectric strength for higher energy density. Simply relying on a moderate increase in dielectric strength in combination with higher dielectric permittivity would lead to a practical solution for a capacitor to be superior.

4.5 | Inconsistent testing set-up

The choice of the electrode geometry can substantially alter the dielectric breakdown of the samples. The fact is that different laboratories use various electrode fixtures and test protocols. The difference includes tip-plane electrode, ball-plane configuration, sphere-sphere configuration, parallel metal plates, metalized film electrodes, and metalized film samples. The sample breakdown is mainly governed by the major flaws inside the sample, on the sample surface, and the adjacency of reinforcing particles, where cautions should be taken for large scale thin film tests.[226,227] Some measurements performed, for instance, in a sphere-sphere configuration, are not very sensitive to variations within the polymeric matrix. Under a divergent field, the field is initially enhanced at the tip of the growing tree during the whole breakdown process. The major flaws might not be reachable by the damaging tree and an increase in breakdown field results. For films with high roughness and pits, the air pockets and gaps between metal electrodes and film surfaces may cause false breakdown phenomena. The breakdown voltages are often over-valued, and the real dielectric strength of the film body is not correctly recorded. This can be the case for filled composite films that are more likely rougher and subject to more air gaps with the electrodes. There is a need to know the sample surface condition, testing fixtures, and film thickness. It is also necessary to develop and use more consistent testing fixtures for increasingly thinner films and to understand their responses toward energizing the electrodes.

5 | CONCLUSIONS AND OUTLOOK

The operational voltage stress is the fundamental design limitation for high voltage systems. The dielectric community has been tirelessly endeavoring to push back the design barriers. Enhancement in dielectric strength of polymers via nanodielectric engineering becomes more apparent and feasible after almost two decades of endeavor. Figure 24b summarizes the various efforts toward dielectric material investigation. Both low-dimensional nanofiller selection and core-shell design are

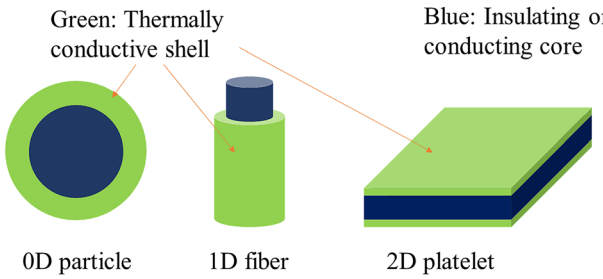

FIGURE 25 Schematic of multifunctional core-shell design integrating thermally conductive shell and electrically insulating or conducting core [Color figure can be viewed at wileyonlinelibrary.com]

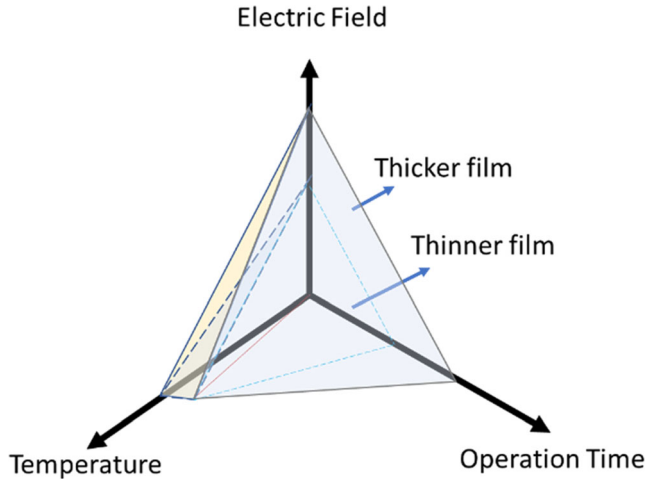

FIGURE 26 Schematic of multiple properties anticipated of a future dielectric material [Color figure can be viewed at wileyonlinelibrary.com]

required to enable this benefit. The filler-polymer interface has become a key ingredient in designing nanodielectric composites capable of enhancing dielectric strength by 46.6% in PVDF/BNNSs composites. It is wise to add low-dimensional fillers at a low loading fraction with an ingenious interface design to realize the contribution of the relevant interfaces. The loading fraction should be maintained below 5 wt%, which leads to high dielectric strength of >600 kV/mm in PVDF composites. In addition, the coupling effects of the filler-polymer interface become an exciting topic, but their impact on the short-term breakdown mechanism is not understood. What is the optimal design using low filler loading and core-shell structure to achieve high dielectric strength? How does it transit from an interface dominating mechanism to a filler dominating with increased filler loading?

Dielectric strength improvement appears to be assisted by thermal management on a nanostructure level. Using highly thermal conducting filling materials, such as BN, AlN, Si_3N_4, etc., turns out preferable for nanodielectric composite engineering. The significant enhancement achieved in high dielectric loss PVDF based composites should be verified and reproduced in low loss polymer systems. Also, a small amount of electrically conducting nanofillers (e.g., Ag, graphene, ZnO, ZnS) appears to suppress electric conductivity by several folds, and to enhance the dielectric strength. One can utilize the synergistic effect of thermally conductive shells and other 2D platelet or 1D fiber or 0D particle as multifunctional core materials (dielectric or conductive) by rational design to achieve a higher dielectric enhancement and energy density (Figure 25). This may be a promising approach to also understand the breakdown mechanism of combined effect of thermal conduction and electrical breakdown.

Inorganic coatings like oxides and nitrides can positively improve dielectric strength and electrical resistivity of polymer and composite films, consequently extending the lifetime of the materials and the device. Depending on the application, a coating layer of several hundreds of nanometers in thickness may enable a further increase in the dielectric strength of both polymer films and polymer-based nanocomposite films by ~30%. Scale-up of roll-to-roll coatings using e-beam and PECVD on free-standing polymer films are feasible and desirable. However, additional investigations should be carried out to understand the impact of coatings on films of various thicknesses and capacitor performance.

Pushing out the voltage rating and heat handling for polymer films with thinner gauge is undoubtedly a good wish (Figure 26). Can a polymer film sustain its high dielectric strength at higher temperature? How does an ultra-thin film respond to an external field? Is it feasible to convert the thin films to practical components with minimal derating in dielectric strength? The ongoing research in the polymer dielectric discipline is basically at the reporting stage of the phenomena. Thorough investigations should understand what materials are superior, how to make them effectively improve the overall dielectric properties, what are the dominating mechanisms in enhancing the properties, and how to utilize phase-field modeling tool to guide the high-performance nanocomposite design. It is anticipated that the genuine and significant increase in dielectric strength is achievable with high consistency on a large number of materials.

ACKNOWLEDGMENTS

This work was financially supported by the Start-up fund of Guangdong Technion Israel Institute of Technology, and Guangdong Basic and Applied Basic Research Foundation—2019A1515012056. The author acknowledges GE dielectric team and Gore dielectric team for various assistance during project execution in the past.

Prof. Richard Siegel from RPI offered technical discussion and manuscript revision.

ORCID

Daniel Q. Tan https://orcid.org/0000-0002-2282-2000

REFERENCES

[1] W. J. Sarjeant, J. Zirnheld, F. W. MacDougall, J. S. Bowers, N. Clark, in *Handbook of Low and High Dielectric Constant Materials and Their Applications*, Vol. 2 (Ed: H. S. Nalwa) Academic Press:, UK **1999**, p. 424.

[2] Office of Basic Energy Science, US Department of Energy, *Basic Research Needs for Electrical Energy Storage*, Office of Basic Energy Science, US Department of Energy, Washington, DC **2007**.

[3] M. L. Sheer, in *Proc. 20th Electrical Electronics Insulation Conf*. Boston, MA 1991, 7–10 October, pp. 181–185.

[4] G. C. Stone, E. A. Boulter, I. Culbert, H. Dhirani, in *Electrical Insulation for Rotating Machines—Design, Evaluation, Aging, Testing, and Repair*, 1st ed. (Ed: S. V. Kartalopoulos), Wiley-IEEE Press, Piscataway, NJ **2004**, p. 73.

[5] J. Han, R. Garrett, *NSTI-Nanotech* **2008**, *2*, 727.

[6] F. MacDougall, J. Ennis, X. H. Yang, K. Seal, S. Phatak, B. Spinks, N. Keller, C. Naruo, T. R. Jow, in *IEEE Explore IEEE Pulsed Power Conf*. **2005**.

[7] S. Adams, F. Macdougall, R. Ellwangar, A. Yializis, *PAPERS – AIAA* **2003**, *21*(5901/6004), 74.

[8] K. Slenes, L. Bragg, in *Int'l Conf. on High Temperature Electronics* 2012, May 8–12, http://www.tplinc.com/uploads/Slenes_HiTEC_2014.pdf (accessed on May 17, 2020).

[9] R. S. Taylor, N. Silvi, Q. Chen, L. L. Zhang, Development, Test and Demonstration of a Cost-Effective, Compact, Light-Weight, and Scalable High Temperature Inverter for HEVs, PHEVs, and FCVs. *DOE report DE-FC26-07NT43121* 2012.

[10] F. J. Wang, D. X. Zhou, Y. X. Hu, *Phys. Status Solidi A* **2009**, *206*(11), 2632. https://doi.org/10.1002/pssa.200925159.

[11] Y. Murata, M. Sakamaki, K. Abe, Y. Inoue, S. Mashio, S. Kashiyam, O. Matsunaga, T. Igi, M. Watanabe, S. Asai, S. Katakai, *SEI Tech. Rev.* **2013**, *76*, 55.

[12] J. C. Fothergill, G. C. Montanari, G. C. Stevens, C. Laurent, G. Teyssedre, L. A. Dissado, U. H. Nilsson, G. Platbrood, *IEEE Trans. Dielectr. Electr. Insul.* **2003**, *10*, 514.

[13] Y. Bai, Z. Y. Cheng, V. Bhatti, H. S. Xu, Q. M. Zhang, *Appl. Phys. Lett.* **2000**, *76*(25), 3804.

[14] S. Beerman-Curtin, *AMMTIAC Q.* **2009**, *4*, 45.

[15] P. H. C. Camargo, K. G. Satyanarayana, F. Wypych, *Mater. Res.* **2009**, *12*, 1.

[16] D. Q. Tan, L. L. Zhang, Q. Chen, P. Irwin, *J. Electron. Mater.* **2014**, *43*, 4569.

[17] J. K. Nelson, J. C. Fothergill, L. A. Dissado, W. Peasgood, in *IEEE Conf. Elect. Insul. Dielec. Phenomena* **2002**, pp. 295–298.

[18] T. Imai, Y. Hirano, H. Hirai, S. Kojima, T. Shimizu, in *IEEE Intern. Sympos. Electr. Insul. (ISEI)*, Boston, MA **2002**, pp. 379–383.

[19] M.-I. Baraton Ed., *Synthesis, Functionalization and Surface Treatment of Nanoparticles*, American Scientific Publishers, Los Angeles, USA **2003**.

[20] Y. Cao, P. C. Irwin, K. Younsi, *IEEE Trans. Dielect. Elect. Insulation* **2004**, *11*, 797.

[21] L. S. Schadler, X. Wang, J. K. Nelson, H. Hillborg, in *Dielectric Polymer Nanocomposites* (Ed: J. K. Nelson), Springer, New York, NY, **2010**, p. 259.

[22] D. Q. Tan, *FY 2014 Advanced Power Electronics and Electric Motors Annual Progress Report*, *US Department of Energy 2014*, https://www.energy.gov/sites/prod/files/2015/04/f21/FY14_EDT_Annual_Report.pdf (accessed: July 2019).

[23] I. Plesa, V. P. Notingher, S. Schlögl, C. Sumereder, M. Muhr, *Polymers* **2016**, *8*, 173.

[24] B. B. Jiang, J. Iocozzia, L. Zhao, H. F. Zhang, Y.-W. Harn, Y. H. Chen, Z. Q. Lin, *Chem. Soc. Rev.* **2019**, *48*, 1194.

[25] E. Baer, L. Zhu, *Macromolecules* **2017**, *50*, 2239.

[26] P. Irwin, W. Zhang, Y. Cao, X. Fang, D. Q. Tan, in *Dielectric Polymer Nanocomposites* (Ed: J. K. Nelson), Springer, New York, NY **2010**, 196, p. 163.

[27] Q. M. Zhang, Giant Electrocaloric Effect In Ferroelectrics With Tailored Polar-Nanostructures report, *DOE Award#: DE-FG02—07ER46410* 2015, The Pennsylvania State University, April 23.

[28] Prateek, V. K. Thakur, R. K. Gupta, *Chem. Rev.* **2016**, *116*, 4260.

[29] Q. Chen, Y. Shen, S. H. Zhang, Q. M. Zhang, *Annu. Rev. Mater. Res.* **2015**, *45*, 433.

[30] W. A. Izzati, Y. Z. Arief, Z. Adzis, M. Shafanizam, *Scientific World Journal* **2014**, *2014*, 735070.

[31] F. N. Musa, N. Bashir, M. H. Ahmad, Z. Buntat, *J. Optoelectron. Adv. M.* **2015**, *17*(3–4), 462.

[32] M. H. Ahmad, N. Bashir, H. Ahmad, A. A. Abd Jamil, A. A. Suleiman, *TELKOMNIKA Indonesian J. Electrical Eng.* **2014**, *12*(8), 5827.

[33] N. H. Ismail, M. Mustapha, *Polym. Eng. Sci.* **2018**, *58*, E36. https://doi.org/10.1002/pen.24822.

[34] L. J. Romasanta, M. A. Lopez-Manchado, R. Verdejo, *Prog. Polym. Sci.* **2015**, *51*, 188.

[35] G. Chen, J. W. Zhao, S. T. Li, L. S. Zhong, *Appl. Phys. Lett.* **2012**, *100*, 222904.

[36] J. Ho, R. Jow, *Army Research Laboratory Report (ARL-TR-4880)*, July 2009, ARL, Adelphi, MD.

[37] D. Q. Tan, High temperature PTFE film for capacitors, *Gore Global Technology Library ID#44438*, December 2018.

[38] D. Q. Tan, *FY 2015 Advanced Power Electronics and Electric Motors Annual Progress Report*, *US Department of Energy* 2015, pp. 221–232, http://energy.gov/eere/vehicles/downloads/vehicle-technologies-office-2015-electric-drive-technologies-annual-rd (accessed: July 2019).

[39] C. Neusel, G. A. Schneider, *J. Mech. Phys. Solids* **2014**, *63*, 201.

[40] Y. Imanaka, T. Shioga, J. D. Baniecki, *FUJITSU Sci. Tech. J.* **2002**, *38*(1), 22.

[41] L. Chen, T. D. Huan, Q. Y. Cardona, R. Ramprasad, *J. Mater. Sci.* **2015**, *51*, 506.

[42] J. Bond, *APEC* 2017, https://www.ecicaps.com/high-temperaturefilm-capacitors/ (accessed: July 2019).

[43] N. Pfeiffenberger, F. Milandou, M. Niemeyer, T. Sugawara, M. Sanner, J. Mahood, *IEEE Trans. Dielectr. Electr. Insul.* **2018**, *25*, 120.

[44] C. M. Kerwien, D. L. Malandro, J. R. Broomall, in *IEEE Conf. Electrical Insulation and Dielectric Phenomena* 2016, October 2016, https://www.gore.com/capacitors.

[45] http://www.sbelectronics.com/2017/05/dupont-teijin-filmsdtf-sbe-announce-collaboration-bring-customers-new-hightemperature-capacitor-technology/ (accessed: July 2019).

[46] Y. Thakur, B. Zhang, R. Dong, W. C. Lu, W. C. Iacob, J. Runt, J. Bernholc, Q. M. Zhang, *Nano Energy* **2017**, *32*, 73.

[47] I. Treufeld, D. H. Wang, B. A. Kurish, L.-S. Tan, L. Zhu, *J. Mater. Chem. A* **2014**, *2*, 20683.

[48] T. C. Chung, *Prog. Polym. Sci.* **2002**, *27*, 39.

[49] X. Yuan, Y. Matsuyama, T. C. Chung, *Macromolecules* **2010**, *43*, 4011.

[50] M. Misra, M. Agarwal, D. W. Sinkovits, S. K. Kumar, C. Wang, G. Pilania, R. Ramprasad, R. A. Weiss, X. Yuan, T. C. M. Chung, *Macromolecules* **2014**, *47*, 1122.

[51] S. Wu, W. Li, M. Lin, Q. Burlingame, Q. Chen, A. Payzant, K. Xiao, Q. M. Zhang, *Adv. Mater.* **2013**, *25*, 1734.

[52] X. Zhang, Y. Shen, Z. H. Shen, J. Y. Jiang, L. Q. Chen, C.-W. Nan, *ACS Appl. Mater. Interfaces* **2016**, *8*, 27236.

[53] A. M. Kanakkithodi, G. M. Treich, T. D. Huan, R. Ma, Y. Cao, G. A. Sotzing, R. Ramprasad, *Adv. Mater.* **2016**, *28*, 6277.

[54] A. F. Baldwin, T. D. Huan, R. Ma, A. M. Kanakkithodi, M. Tefferi, J. E. Marszalek, N. Katz, Y. Cao, R. Ramprasad, G. A. Sotzing, *Macromolecules* **2015**, *48*, 2422.

[55] T. D. Huan, A. M. Kanakkithodi, R. Ramprasad, G. A. Sotzing, *Phys. Rev. B* **2015**, *92*, 014106.

[56] A. M. Kanakkithodi, A. Chandrasekaran, C. Kim, T. D. Huan, G. Pilania, V. Botu, R. Ramprasad, *Mater. Today* **2018**, *21*, 785.

[57] E. A. Stefanescu, X. Tan, Z. Lin, N. Bowler, M. R. Kessler, *Polymer* **2010**, *51*(24), 5823.

[58] T. Zhang, X. Chen, Y. Thakur, B. Lu, Q. Zhang, J. Runt, Q. M. Zhang, *Sci. Adv.* **2020**, *6*(4), eaax6622.

[59] J. Ho, T. R. Jow, S. A. Boggs, *IEEE Trans. Dielectr. Electr. Insul.* **2008**, *15*, 1754.

[60] Z.-M. Dang, J.-K. Yuan, S.-H. Yao, R.-J. Liao, *Adv. Mater.* **2013**, *25*, 6334.

[61] A. Yializis, *FY 2015 Advanced Power Electronics and Electric Motors Annual Progress Report*, *US Department of Energy* 2015, http://energy.gov/eere/vehicles/downloads/vehicle-technologies-office-2015-electricdrive-technologies-annual-rd (accessed: July 2019).

[62] H. Sundstrand, S. Dearborn, Brady, High temperature FPE film capacitors, *Program Report 2007*, March 12, US Dept of Energy DE-FC26-06NT42949, https://digital.library.unt.edu/ark:/67531/metadc838282/ (accessed: July 2019).

[63] Z. Zhou, J. Carr, M. Mackey, K. Yin, D. Schuele, L. Zhu, E. Baer, *J. Polym. Sci. B* **2013**, *51*, 978.

[64] S. O. Kasap, *Principles of Electronic Materials and Devices*, 4th ed., McGraw-Hill Education, New York, NY **2018**.

[65] H. R. Zeller, P. Pfluger, J. Bernasconi, *IEEE Trans. Electrical Insulation* **1984**, *EI-9*(3), 200. https://doi.org/10.1109/TEI.1984.298747.

[66] P. P. Budenstein, Dielectric breakdown in solids, AD-AO12 177, *Technical Report RG-75-25 Army Missile Research*, Development and Engineering Laboratory, Redstone Arsenal, Alabama, 1974, 20 December.

[67] S. L. Nunes, M. T. Shaw, *IEEE Trans. Electrical Insulation* **1980**, *EI-15*(6), 437.

[68] M. Ieda, *IEEE Trans. Electrical Insulation* **1980**, *EI-15*(3), 206.

[69] M. Hikita, T. Hirose, Y. Ito, T. Mizutani, M. Ieda, *J. Phys. D: Appl. Phys.* **1990**, *23*, 1515.

[70] H.-Z. Ding, X.-S. Xing, H.-S. Zhu, *J. Phys. D: Appl. Phys.* **1994**, *27*, 591.

[71] M. Ieda, M. Nagao, M. Hikita, *IEEE Trans. Dielectrics Electrical Insulation* **1994**, *1*(5), 934.

[72] A.N. Hammoud, E. D. Baumarm, E. Overton, I. T. Myers, J. L. Suthar, W. Khachen, J. R. Laghari, in *Conf. Electrical Insulation Dielectric Phenomena*, Annual report, October 1992, pp. 549–554.

[73] J. J. Huang, Y. Zhang, T. Ma, H. T. Li, L. W. Zhang, *Appl. Phys. Lett.* **2010**, *96*, 042902.

[74] Y. Cao, P. C. Irwin, in *Proc. Conf. Electrical Insulation Dielectric Phenomena (CEIDP)* **2003** October, Albuquerque, NW, pp. 19–22; pp. 116–119.

[75] D. Q. Tan, Y. Cao, E. Tuncer, P. Irwin, *Mater. Sci. Appl.* **2013**, *4*, 6.

[76] Q. Tan, Y. Cao, P. Irwin, in *Proc. 2007 IEEE Int. Conf. Solid Dielectrics (ICSD)* **2007**, Winchester, UK.

[77] Z.-M. Dang, J.-K. Yuan, J.-W. Zha, T. Zhou, S.-T. Li, G.-H. Hu, *Prog. Mater. Sci.* **2012**, *57*, 660.

[78] Q. H. Lin, S. A. Cohen, L. Gignac, B. Herbst, D. Klaus, E. Simonyi, J. Hedricj, J. Warlaumont, H.-J. Lee, W.-L. Wu, *J. Polym. Sci. Part B: Polym. Phys.* **2007**, *45*, 1482.

[79] M. Roy, J. K. Nelson, R. K. MacCrone, L. S. Schadler, C. W. Reed, R. Keefe, *IEEE Trans. Dielectr. Electr. Insul.* **2005**, *12*, 629.

[80] H. Yahyaoui, P. Notingher, S. Agnel, C. Perrier, Y. Kieffel, *2016 IEEE Int. Conf. Dielectrics (ICD)* **2016**, 978-1-5090-2804-7/16/.

[81] C. Calebrese, L. Hui, L. S. Schadler, J. K. Nelson, *IEEE Trans. Dielectr. Electr. Insul.* **2011**, *18*, 938.

[82] T. Tanaka, G. C. Montanari, R. Mülhaupt, *IEEE Trans. Dielectr. Electr. Insul.* **2004**, *11*, 763.

[83] E. Tuncer, I. Sauers, D. R. James, A. R. Ellis, A. Goyal, K. L. More, *Nanotechnology* **2007**, *18*, 1.

[84] S. T. Li, S. H. Yu, Y. Feng, *High Volt.* **2016**, *1*(3), 122.

[85] Y. Luo, G. N. Wu, J. W. Liu, G. Y. Zhu, P. Wang, J. Peng, K. J. Cao, *IEEE Trans. Dielectrics Electrical Insulation* **2014**, *21*(5), 2237.

[86] I. Plesa, P. V. Notingher, C. Stancu, F. Wiesbrock, S. Schlögl, *Polymers* **2019**, *11*, 24. https://doi.org/10.3390/polym11010024.

[87] X. Huang, P. Jiang, T. A. Tanaka, *IEEE Electr. Insul. Mag.* **2011**, *27*, 8.

[88] T. Andritsch, R. Kochetov, Y. T. Gebrekiros, P. H. F. Morshuis, J. J. Smit, in *Proc. Int'l Conf. Solid Dielectrics (ICSD)* **2010**, Postdam, Germany, pp. 1–4.

[89] T. H. Lee, S. B. Lee, J. H. Nam, Y. H. Kim, S. K. Lee, I. H. Lee, S. I. Jeon, Y. J. Won, J. S. Kim, J. H. Lee, in *Proc. CIGRE Session* **2014**, Paris, France, pp. 24–29.

[90] A. S. Paramane, K. S. Kumar, *Trans. Electrical Electronic Mater.* **2016**, *17*(5), 239.

[91] S. Li, G. Yin, G. Chen, J. Li, S. Bai, L. Zhong, Y. Zhang, Q. Lei, *IEEE Trans. Dielectr. Electr. Insul.* **2010**, *17*, 1523.

[92] Y. J. Hu, R. C. Smith, J. K. Nelson, L. S. Schadler, in *IEEE Conf. Electr. Insul. Dielectr. Phenomena (CEIDP)* **2006**, pp. 31–34.

[93] Y. Murakami, M. Nemoto, S. Okuzumi, S. Masuda, M. Nagao, *IEEE Trans. Dielectr. Electr. Insul.* **2008**, *15*, 33.

[94] S. Okuzumi, Y. Murakami, M. Nagao, Y. Sekiguchi, C. C. Reddy, Y. Murata, in *IEEE Conf. Electr. Insul. Dielectr. Phenomena (CEIDP)* **2008**, pp. 722–725.
[95] J. K. Nelson, J. C. Fothergill, *Nanotechnology* **2004**, *15*, 586.
[96] Y. Yin, X. B. Dong, Z. Li, X. G. Li, in *IEEE Intern. Conf. Solid Dielectrics* **2007**, pp. 372–376.
[97] C. Zilg, D. Kaempfer, R. Thomann, R. Muelhaupt, G. C. Montanari, *IEEE Conf. Electr. Insul. Dielectr. Phenomena (CEIDP)* **2003**, pp. 546–550.
[98] Q. Wang, G. Chen, *Adv. Mater. Res.* **2012**, *1*, 93.
[99] S. Singha, M. J. Thomas, *IEEE Trans. Dielectr. Electr. Insul.* **2008**, *15*, 12.
[100] T. Imai, F. Sawa, T. Nakano, T. Ozaki, T. Shimizu, M. Kozako, T. Tanaka, *IEEE Trans. Dielectr. Electr. Insul.* **2006**, *13*, 319.
[101] K. Y. Lau, A. S. Vaughan, G. Chen, I. L. Hosier, A. F. Holt, K. Y. Ching, *IEEE Trans. Dielectr. Electr. Insul.* **2014**, *21*, 340.
[102] K. Y. Lau, A. S. Vaughan, G. Chen, *IEEE Electr. Insul. Mag.* **2015**, *31*, 45.
[103] Y. Shen, Y. Lin, C. W. Nan, *Adv. Funct. Mater.* **2007**, *17*, 2405.
[104] Y. Shen, Y. H. Lin, M. Li, C. W. Nan, *Adv. Mater.* **2007**, *19*, 1418.
[105] D. Pitsa, M. Danikas, *Nano Brief Rep. Rev.* **2011**, *6*(6), 497. https://doi.org/10.1142/S1793292011002949.
[106] L. Schadler, *Nat. Mater.* **2007**, *6*, 257.
[107] S. F. Mendes, C. M. Costa, C. Caparrós, V. Sencadas, S. Lanceros-Méndez, *J. Mater. Sci.* **2012**, *47*, 1378.
[108] J. Li, *Phys. Rev. Lett.* **2003**, *90*, 217601.
[109] F. He, S. Lau, H. L. Chan, J. Fan, *Adv. Mater.* **2009**, *21*, 710.
[110] S. M. Peng, X. Yang, Y. Yang, S. J. Wang, Y. Zhou, J. Hu, Q. Li, J. L. He, *Adv. Mater.* **2019**, *31*, 1807722.
[111] S. M. Peng, Q. B. Zeng, X. Yang, J. Hui, X. H. Qiu, J. L. He, *Sci. Rep.* **2016**, *6*, 38978.
[112] R. D. Averitt, S. L. Westcott, N. J. Halas, *J. Opt. Soc. Am. B* **1999**, *16*, 1824.
[113] J.-W. Ha, I. J. Park, S.-B. Lee, D.-K. Kim, *Macromolecules* **2002**, *35*, 6811.
[114] R. A. Ramil, W. A. Laftah, S. Hashim, *RSC Adv.* **2013**, *3*, 15543.
[115] Y. U. Wang, D. Q. Tan, J. Krahn, *J. Appl. Phys.* **2011**, *110*, 044103.
[116] K. Yu, Y. Niu, Y. Bai, Y. Zhou, H. Wang, *Appl. Phys. Lett.* **2013**, *102*, 102903.
[117] G. Wang, Y. Huang, Y. Wang, P. Jiang, X. Huang, *Phys. Chem. Chem. Phys.* **2017**, *19*, 21058.
[118] Z. Li, L. A. Fredin, P. Tewari, S. A. DiBenedetto, M. T. Lanagan, M. A. Ratner, T. J. Marks, *Chem. Mater.* **2010**, *22*, 5154.
[119] M. Xanthos, in *Functional Fillers for Plastics*, 2nd ed. (Ed: M. Xanthos), Wiley-VCH Verlag GmbH & Co. KGaA, Weinheim, Germany **2010**, p. 1.
[120] M. D. Marquis, E. Guillaume, C. Chivas-Joly, in *Nanocomposites and Polymers with Analytical Methods* (Ed: J. Cuppoletti), InTech, Rijeka, Croatia **2011**, p. 261.
[121] J. Li, P. Khanchaitit, K. Han, Q. Wang, *Chem. Mater.* **2010**, *22*, 5350.
[122] G. Wang, X. Huang, P. Jiang, *ACS Appl. Mater. Interfaces* **2015**, *7*, 18017.
[123] Y. Deng, Y. Zhang, Y. Xiang, G. Wang, H. Xu, *J. Mater. Chem.* **2009**, *19*, 2058.
[124] M. Rahimabady, M. S. Mirshekarloo, K. Yao, L. Lu, *Phys. Chem. Chem. Phys.* **2013**, *15*, 16242.
[125] H. M. Jung, J. H. Kang, S. Y. Yang, J. C. Won, Y. S. Kim, *Chem. Mater.* **2010**, *22*, 450.
[126] J. W. Xu, C. P. Wong, *Appl. Phys. Lett.* **2005**, *87*, 082907.
[127] C. Yang, Y. H. Lin, C. W. Nan, *Carbon* **2009**, *47*, 1096.
[128] L. X. He, S. C. Tong, *eXPRESS Polym. Lett.* **2013**, *7*(4), 375.
[129] J. Chen, X. Wang, X. Yu, L. Yao, Z. Duan, Y. Fan, Y. Jiang, Y. Zhou, Z. Pan, *J. Mater. Chem. C* **2018**, *6*, 271.
[130] Z. L. Li, B. X. Du, C. L. Han, H. Xu, *Sci. Rep.* **2017**, *7*, 4015.
[131] S. J. Ding, S. H. Yu, X. D. Zhu, S. H. Xie, R. Sun, W.-H. Liao, C.-P. Wong, *Appl. Phys. Lett.* **2017**, *111*, 153902.
[132] M. Matsuoka, *Jpn. J. Appl. Phys.* **1971**, *10*, 736.
[133] K. Eda, *IEEE Electr. Insul. M.* **1989**, *5*(6), 28.
[134] Y. Sato, T. Yamamoto, Y. Ikuhara, *J. Am. Ceram. Soc.* **2007**, *90*(2), 337.
[135] J. Glatz-Reichenbach, B. Meyer, R. Strompler, P. Kluge-Weiss, F. Greuter, *J. Mater. Sci.* **1996**, *31*, 5941.
[136] D. Q. Tan, P. A. Irwin, W. Zhang, US Patent, *8,421,045 B2*, **2016**.
[137] X. Yang, X. L. Zhao, J. L. He, *IEEE Electr. Insul. M.* **2018**, *34* (1), 16.
[138] A. Shamsi, I. Kazeminezhad, S. M. Aref, A. Kiasat, *Curr. Nanosci.* **2017**, *13*(2), 175.
[139] D. Q. Tan, *Int. J. Ceramic Eng. Sci.* **2019**, *1*, 136. https://doi.org/10.1002/ces2.10017.
[140] C. C. Ma, H.-C. Kuan, Y.-J. Chen, *J. Appl. Polym. Sci.* **2006**, *100*(1), 508.
[141] N. Soltani, A. Dehzangi, A. Kharazmi, E. Saion, W. Mahmood, M. Yunus, B. Y. Majlis, M. Zare, E. Gharibshahi, N. Khalilzadeh, *Chalcogenide Lett.* **2014**, *11* (2), 79.
[142] S. J. Ding, Y. M. Kong, *ACS Appl. Electron. Mater.* **2019**, *1*, 1752.
[143] S. B. Luo, J. Y. Yu, S. H. Yu, R. Sun, L. Cao, W.-H. Liao, C.-P. Wong, *Adv. Energy Mater.* **2019**, *9*, 1803204.
[144] S. H. Yu, S. J. Ding, D. Q. Tan, J. Y. Yu, Y. C. Lu, R. Sun, J. B. Xu, C.-P. Wong, personal communication, **2019**.
[145] Y. U. Wang, D. Q. Tan, *J. Appl. Phys.* **2011**, *109*, 104102.
[146] X. Y. Huang, B. Sun, Y. K. Zhu, S. T. Li, P. K. Jiang, *Prog. Mater. Sci.* **2018**, *100*, 187.
[147] Z. P. Wang, J. K. Nelson, J. J. Miao, R. J. Linhardt, L. S. Schadler, H. Hillborg, S. Zhao, *IEEE Trans. Dielectrics Electrical Insulation* **2012**, *19*(3), 960.
[148] H. Tang, Y. R. Lin, H. A. Sodano, *Adv. Energy Mater.* **2012**, *2*, 469.
[149] H. Tang, Y. R. Lin, C. Andrew, H. A. Sodano, *Nanotechnology* **2011**, *22*, 015702.
[150] C. Pecharroman, F. Esteban-Betegon, J. F. Bartolome, S. Lopez-Esteban, J. S. Moya, *Adv. Mater.* **2001**, *13*, 1541.
[151] C. W. Nan, Y. Shen, J. Ma, *Annu. Rev. Mater. Res.* **2010**, *40*, 131.
[152] Q. Li, K. Han, M. R. Gadinski, G. Zhang, Q. Wang, *Adv. Mater.* **2014**, *26*, 6244.
[153] Q. Li, L. Chen, M. R. Gadinski, S. Zhang, G. Zhang, H. U. Li, E. Iagodkine, A. Haque, L.-Q. Chen, T. N. Jackson, Q. Wang, *Nature* **2015**, *523*, 576.
[154] S. P. Fillery, H. Koerner, L. Drummy, E. Dunkerley, M. F. Durstock, *ACS Appl. Mater. Interfaces* **2012**, *4*, 1388.

[155] Z.-H. Shen, J.-J. Wang, Y. Lin, C.-W. Nan, L.-Q. Chen, Y. Shen, *Adv. Mater.* **2017**, *30*, 1704380.
[156] D. Kang, G. Wang, Y. Huang, P. Jiang, X. Huang, *ACS Appl. Mater. Interfaces* **2018**, *10*, 4077.
[157] Y. Song, Y. Shen, H. Y. Liu, Y. H. Lin, M. Li, C. W. Nan, *J. Mater. Chem.* **2012**, *22*, 16491.
[158] X. Zhang, J. Jiang, Z. Shen, Z. Dan, M. Li, Y. Lin, *Adv. Mater.* **2018**, *30*, 1707269.
[159] Z. Pan, J. Zhai, B. Shen, *J. Mater. Chem. A* **2017**, *5*, 15217.
[160] X. Zhang, B.-W. Li, L. J. Dong, H. X. Liu, W. Chen, Y. Shen, C.-W. Nan, *Adv. Mater. Interfaces* **2018**, *5*(11), 1800096.
[161] I. Ozsoy, A. Demirkol, A. Mimaroglu, H. Unal, Z. Demir, *J. Mech. Eng.* **2015**, *61*, 601.
[162] Q. Li, G. Zhang, F. Liu, K. Han, M. R. Gadinski, C. Xiong, Q. Wang, *Energy Environ. Sci.* **2015**, *8*, 922.
[163] X. Zhu, S. Luo, S. Yu, B. Chu, R. Sun, C.-P. Wong, in *2018 19th Int. Conf. Electronic Packaging Technology (ICEPT)* **2018**.
[164] Q. Li, F. Liu, T. Yang, M. R. Gadinski, G. Zhang, L. Q. Chen, Q. Wang, *Proc. Natl. Acad. Sci. USA* **2016**, *113*, 9995.
[165] L. Wu, K. Wu, C. Lei, D. Liu, R. Du, F. Chen, Q. Fu, *J. Mater. Chem. A* **2019**, *7*, 7664. https://doi.org/10.1039/C9TA00616H.
[166] S. Kango, S. Kalia, A. Celli, J. Njuguna, Y. Habibi, R. Kumar, *Prog. Polym. Sci.* **2013**, *38*, 1232.
[167] S. Mallakpour, M. Madani, *Prog. Org. Coat.* **2015**, *86*, 194.
[168] H. Luo, H. F. Zhou, C. Ellingford, Y. Zhang, S. Chen, K. C. Zhou, D. Zhang, C. R. Bowen, C. Y. Wan, *RSC Chem. Soc. Rev.* **2019**, *48*, 4424.
[169] Q. Wang, L. Zhu, *J. Polym. Sci. Part B: Polym. Phys.* **2011**, *49*, 1421.
[170] F. Lin, *Master Thesis*. University of Waterloo, Ontario, Canada, **2006**, p. 160.
[171] M. Sabzi, S. M. Mirabedini, J. Zohuriaan-Mehr, M. Atai, *Prog. Org. Coat.* **2009**, *65*, 222.
[172] P. Tao, A. Viswanath, Y. Li, R. W. Siegel, B. C. Benicewicz, L. S. Schadler, *Polymer* **2013**, *54*, 1639.
[173] R. W. Siegel, S. K. Chang, B. J. Ash, J. A. P. M. Stone, R. W. Doremus, L. S. Schadler, *Scr. Mater.* **2001**, *44*, 2061.
[174] H. Lee, S. M. Dellatore, W. M. Miller, P. B. Messersmith, *Science* **2007**, *318*, 426.
[175] Y. Song, Y. Shen, H. Liu, Y. Lin, M. Li, C.-W. Nan, *J. Mater. Chem.* **2012**, *22*, 8063.
[176] P. Hu, L. Yan, C. Zhao, Y. Zhang, J. Niu, *Compos. Sci. Technol.* **2018**, *168*, 327.
[177] B. Balasubramanian, K. L. Kraemer, N. L. Reding, R. Skomski, S. Ducharme, D. J. Sellmyer, *ACS Nano* **2010**, *4* (4), 1893.
[178] Q. J. Cai, Y. Gan, M. B. Chan-Park, H. B. Yang, Z. S. Lu, Q. L. Song, C. M. Li, Z. L. Dong, *Appl. Phys. Lett.* **2008**, *93*, 113304.
[179] Z. Ahmad, *InTechOpen*. https://www.intechopen.com/books/dielectric-material/polymer-dielectric-materials (accessed: October 3, 2012).
[180] H. T. Vo, F. G. Shi, *Microelectron. J.* **2002**, *33*, 409.
[181] Y. Kim, M. Kathaperumal, V. W. Chen, Y. Park, C. Fuentes-Hernandez, M. J. Pan, B. Kippelen, J. W. Perry, *Adv. Energy Mater.* **2015**, *5*, 1500767.
[182] J. O. Zoppe, N. C. Ataman, P. Mocny, J. Wang, J. Moraes, H.-A. Klok, *Chem. Rev.* **2017**, *117*, 1105.
[183] X. Huang, P. Jiang, *Adv. Mater.* **2015**, *27*, 546.
[184] H. Luo, D. Zhang, C. Jiang, X. Yuan, C. Chen, K. Zhou, *ACS Appl. Mater. Interfaces* **2015**, *7*, 8061.
[185] A. Toor, H. Y. So, A. P. Pisano, *ACS Appl. Mater. Interfaces* **2017**, *9*, 6369.
[186] K. Yang, X. Huang, Y. Huang, L. Xie, P. Jiang, *Chem. Mater.* **2013**, *25*, 2327.
[187] P. Kim, S. C. Jones, P. J. Hotchkiss, J. N. Haddock, B. Kippelen, S. R. Marder, J. W. Perry, *Adv. Mater.* **2007**, *19*, 1001.
[188] G. Q. Zhang, D. Brannum, D. X. Dong, L. X. Tang, L. Allahyarov, S. Tang, K. Kodweis, J.-K. Lee, L. Zhu, *Chem. Mater.* **2016**, *28*, 4646.
[189] Y. C. Xie, Y. Y. Yu, Y. F. Feng, W. R. Jiang, Z. C. Zhang, *ACS Appl. Mater. Interfaces* **2017**, *9*, 2995.
[190] R. Prateek, S. Bhunia, A. G. Siddiqui, R. K. Gupta, *ACS Appl. Mater. Interfaces* **2019**, *11*, 14329.
[191] C. A. Grabowski, S. P. Fillery, H. Koerner, M. Tchoul, L. Drummy, C. W. Beier, R. L. Brutchey, M. F. Durstock, R. L. Vaia, *Nanocomposites* **2016**, *2*, 117. https://doi.org/10.1080/20550324.2016.1223913.
[192] M. N. Tchoul, S. P. Fillery, H. Koerner, L. F. Drummy, F. T. Oyerokun, P. A. Mirau, M. F. Durstock, R. A. Vaia, *Chem. Mater.* **2010**, *22*, 1749. https://doi.org/10.1021/cm903182n.
[193] H. Luo, C. Ma, X. Zhou, S. Chen, D. Zhang, *Macromolecules* **2017**, *50*, 5132.
[194] H. Luo, S. Chen, L. H. Liu, X. F. Zhou, C. Ma, W. W. Liu, D. Zhang, *ACS Sustainable Chem. Eng.* **2019**, *7*, 3145.
[195] A. Yializis, G. L. Powers, D. G. Shaw, *IEEE Trans. Comp. Hybrids Manuf. Technol.* **1990**, *13*, 611.
[196] D. Q. Tan, G. T. Dalakos, Y. Cao, Q. Chen, R. A. Zhao, *US Patent*, 8354166 **2011**.
[197] D. Q. Tan, P. C. Irwin, G. T. Dalakos, Y. Cao, *US Patent*, 8,094,431 **2010**.
[198] J. Sullivan, *FY 2016 Advanced Power Electronics and Electric Motors Annual Progress Report US DOE* 2016, https://www.energy.gov/sites/prod/files/2017/08/f36/FY16%20EDT%20Annual%20Report_FINAL.pdf (accessed: July 2019).
[199] H. Q. Lu, H. Cui, I. Bhat, S. Murarka, W.-J. Hsia, W. D. Li, *J. Vac. Sci. Technol. B* **2002**, *20*(3), 828.
[200] A. Ismach, H. Chou, D. A. Ferrer, Y. Wu, S. McDonnell, H. C. Floresca, A. Covacevich, C. Pope, R. Piner, M. J. Kim, R. M. Wallace, L. Colombo, R. S. Ruoff, *ACS Nano* **2012**, *6*, 6378.
[201] K. K. Kim, A. Hsu, X. Jia, S. M. Kim, Y. Shi, M. Dresselhaus, T. Palacios, J. Kong, *ACS Nano* **2012**, *6*, 8583.
[202] X. Zhou, Q. Chen, Q. M. Zhang, S. Zhang, *IEEE Trans. Dielectr. Electr. Insul.* **2011**, *18*(2), 463.
[203] Y. Zhou, Q. Li, B. Dang, Y. Yang, T. Shao, H. Li, J. Hu, R. Zeng, J. L. He, Q. Wang, *Adv. Mater.* **2018**, *30*, 1805672.
[204] A. Aziz, M. R. Gadinski, Q. Li, M. A. AlSaud, J. J. Wang, Y. Wang, B. Wang, F. H. Liu, L.-Q. Chen, N. Alem, Q. Wang, *Ad. Mater.* **2017**, *29*, 1701864.
[205] H. Luo, D. Zhang, L. Wang, C. Chen, J. Zhou, K. Zhou, *RSC Adv.* **2015**, *5*, 52809.
[206] Y. Wang, L. Wang, Q. Yuan, Y. Niu, J. Chen, Q. Wang, H. Wang, *J. Mater. Chem. A* **2017**, *5*, 10849.
[207] Y. F. Wang, J. Cui, Q. B. Yuan, Y. J. Niu, Y. Y. Bai, H. Wang, *Adv. Mater.* **2015**, *27*, 6658.
[208] L. Zhu, *J. Phys. Chem. Lett.* **2014**, *5*, 3677. https://doi.org/10.1021/jz501831q.

[209] M. Mackey, D. E. Schuele, L. Zhu, L. Flandin, M. A. Wolak, J. S. Shirk, A. Hiltner, E. Baer, *Macromolecules* **2012**, *45*, 1954.
[210] Z. Zhang, D. H. Wang, M. H. Litt, L.-S. Tan, L. Zhu, *Angew. Chem. Int. Ed.* **2018**, *57*, 1528.
[211] J.-K. Tseng, S. Tang, Z. Zhou, M. Mackey, J. M. Carr, R. Mu, L. Flandin, D. E. Schuele, E. Baer, L. Zhu, *Polymer* **2014**, *55*, 8.
[212] F.-C. Chiu, *Adv. Mater. Sci. Eng.* **2014**, *2014*, 578168. https://doi.org/10.1155/2014/578168.
[213] P. Solomon, *J. Vac. Sci. Technol.* **1977**, *14*, 1122. https://doi.org/10.1116/1.569344.
[214] S. Lombardo, J. H. Stathis, B. P. Linder, K. L. Pey, F. Palumbo, *J. Appl. Phys.* **2005**, *98*, 121301. https://doi.org/10.1063/1.2147714.
[215] M. G. Danikas, T. Tanaka, *IEEE Electr. Insul. M.* **2009**, *25*(4), 19.
[216] Y. Cao, Innovative mica and BN tapes for generator application, *GE Internal Report* **2011**.
[217] J. Wang, Yu, Y. C. Xie, J. J. Liu, Z. C. Zhang, Q. Zhuang, J. Kong, *Polymers* **2018**, *10*, 1349.
[218] K. Mimura, Y. Nakamura, M. Masaki, T. Nishimura, *J. Photopolymer Sci. Technol.* **2015**, *28*(2), 169.
[219] R. Kochetov, T. Andritsch, U. Lafont, P. H. F. Morshuis, S. J. Picken, J. J. Smit, in *Proc. IEEE Electrical Insulation Conf. (EIC)* 2009, 31 May–June 3, Montreal, QC, Canada, pp. 524–528.
[220] Z.-H. Shen, J.-J. Wang, J.-Y. Jiang, Y.-H. Lin, C.-W. Nan, L.-Q. Chen, Y. Shen, *Adv. Energy Mater.* **2018**, *8*, 1800509.
[221] Z. Han, J. W. Wood, H. Herman, C. Zhang, G. C. Stevens, in *Proc. IEEE Int. Symposium Electrical Insulation (ISEI)* **2008**, 9–12 June, Vancouver, BC, Canada, pp. 497–501.
[222] Y. S. Xu, D. D. L. Chung, *Compos. Interfaces* **2000**, *7*, 243.
[223] T. R. Jow, P. J. Cygan, in *Conf. Record 1992 IEEE Int. Symposium Electrical Insulation* **1992**, 7–10 June, Baltimore, MD.
[224] S. H. Zhang, PVDF resin and film properties, www.PolyKtechnologies.com, June 2019.
[225] T. Andritsch, R. Kochetov, Y. T. Gebrekiros, U. Lafont, P. H. F. Morshuis, J. J. Smit, in *Proc. IEEE Conf. Electrical Insulation and Dielectric Phenomena (CEIDP)* **2009**, 18–21 October, Virginia Beach, VA, pp. 523–526.
[226] D. Q. Tan, *Adv. Funct. Mater.* **2019**, *30*, 1808567.
[227] D. Q. Tan, *IET Nanodielectr.* **2020**, *3*(1), 28.
[228] M. T. Lanagan, personal communication, **2006**.

AUTHOR BIOGRAPHY

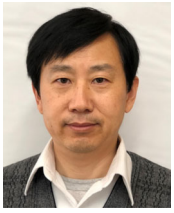

Daniel Q. Tan earned his Ph.D. in Solid State Physics from Chinese Academy of Science in 1989, and Ph. D. in Materials Science and Engineering from University of Illinois at Urban-Champaign in 1998. After working at Honeywell, CTS Corporation, GE Global Research and W.L. Gore for 20 years in USA, he joined Guangdong Technion Israel Institute of Technology at a faculty in 2018. His research interests include the energy storage materials, nanodielectric thin film, piezoelectric and microwave dielectrics, modified organic membranes.

How to cite this article: Tan DQ. The search for enhanced dielectric strength of polymer-based dielectrics: A focused review on polymer nanocomposites. *J Appl Polym Sci*. 2020;e49379. https://doi.org/10.1002/app.49379